Research Square

Preprints are preliminary reports that have not undergone peer review.
They should not be considered conclusive, used to inform clinical practice,
or referenced by the media as validated information.

Bioprospecting and characterization of Trichoderma and Bacillus species as biocontrol agents against Macrophomina phaseolina in maize

Jayne Deboni da Veiga
Fábio Antônio Antonelo
Arthur Germano Fett-Neto
Andréia Mara Rotta de Oliveira
André Costa da Silva

andrecs@ufrgs.br

Universidade Federal do Rio Grande do Sul https://orcid.org/0000-0001-5505-7678

Research Article

Keywords: Biological control, Resistance induction, Charcoal rot, Growth promotion, Seed treatment, Zea mays L

Posted Date: September 29th, 2026

DOI: https://doi.org/10.21203/rs.3.rs-10451624/v1

License: This work is licensed under a Creative Commons Attribution 4.0 International License. Read Full License

Abstract

Macrophomina phaseolina is a soil-dwelling fungus that causes charcoal rot in maize. Its wide host range, microsclerotia formation, and the lack of effective chemical control and resistant maize genotypes make it a major agricultural challenge. This study aimed to identify potential biological control agents (BCAs) against *M. phaseolina* and elucidate their mechanisms of action. An initial in vitro bioprospecting was performed using 59 bacterial and fungal isolates. Selected isolates were characterized for direct antagonism, antibiosis mediated by volatile (VOCs) and non-volatile compounds (NVOCs), hyperparasitism, growth promotion in maize seedlings, and induction of antioxidant and defense responses through modulation of catalase (CAT), superoxide dismutase (SOD), and phenylalanine ammonia-lyase (PAL). *Trichoderma harzianum* (CCT 7589), *T. asperellum* (ASN 60), *Bacillus velezensis* (OQ268070.1), and *B. subtilis amyloliquefaciens* (ASN 09) significantly inhibited *M. phaseolina* mycelial growth. *Trichoderma* isolates exhibited strong hyperparasitism, competition for space and nutrients, and antibiosis via VOCs and NVOCs, whereas *Bacillus* isolates showed greater antibiosis mediated by both compounds. All BCAs increased root biomass in healthy maize seedlings, while only *T. harzianum* and *B. velezensis* also enhanced shoot biomass. The BCAs also modulated antioxidant and defense responses: CAT activity increased following treatment with *T. harzianum* and *B. velezensis*, SOD activity was enhanced by *T. asperellum*, *T. harzianum*, and *B. velezensis*, and PAL activity by *B. subtilis amyloliquefaciens* and *B. velezensis*. These findings indicate that the efficacy of *Trichoderma* and *Bacillus* isolates against *M. phaseolina* results from the integration of direct antagonism, plant growth promotion, and modulation of biochemical defense responses in maize seedlings.

1. Introduction

Macrophomina phaseolina (Tassi) Goid (Goidanich, 1947), the causal agent of smut rot in maize, is a cosmopolitan soil fungus with high ecological plasticity (Harlapur et al., 2024). This fungus is capable of infecting more than 500 plant species and producing highly resistant microsclerotia, which can remain viable in the soil for up to 15 years (Marquez et al., 2021). In maize (*Zea mays* L.), the disease severely compromises growth and biomass accumulation, especially under conditions of water deficit and high temperatures (Harlapur et al., 2024; Khalili et al., 2026). Its management is hampered by the absence of registered fungicides, the low effectiveness of crop rotation, and the absence of resistant commercial genotypes (Harlapur et al., 2024; Agrofit, 2026; Khalili et al., 2026).

Biological control agents (BCAs) have been investigated as a promising alternative for managing soil-borne phytopathogens in different crops (Chauhan et al., 2022; Ahmed & Shoiab, 2024; Veiga et al., 2026). The efficacy of these agents is associated with the functional integration between direct antagonism mechanisms, such as antibiosis mediated by antimicrobial metabolites, competition, and hyperparasitism (Marquez et al., 2021; Veiga et al., 2026), as well as in the activation of biochemical and structural defense responses in plants (Luo et al., 2022; Poria et al., 2025). However, the relative contribution of these mechanisms varies between species and even between isolates of the same species of BCAs (Ghanbarzadeh et al. 2014; Jayanti et al., 2025).

Although *Pseudomonas syringae* has shown potential to reduce the severity of charcoal rot in maize (Ahmed & Shoiab, 2024), and several BCAs have been reported as inducers of defense mechanisms in different crops against *M. phaseolina* (Chauhan, *et al*., 2022; Poria et al., 2025), there are still gaps in the identification of promising new agents and in elucidating the mechanisms involved in suppressing this pathogen in maize. Most studies focus on the effectiveness of biological control, with less emphasis on characterizing the mechanisms of direct antagonism and modulating the biochemical defense responses of the host. Furthermore, little is known about the interaction between these mechanisms when the agents are applied via seed treatment, especially during the early stages of colonization and seedling establishment.

This study is based on the hypothesis that different species of bacterial and fungal agents (BCAs) have potential for controlling *M. phaseolina* in maize, acting through complementary mechanisms such as direct antagonism, production of antifungal metabolites, induction of biochemical defense responses, and promotion of maize seedling growth. Thus, the objectives of this study were: (i) to evaluate *in vitro* the antagonistic potential of 59 bacterial and fungal isolates against *M. phaseolina*; (ii) to select promising BCAs; (iii) to characterize the main mechanisms of action of the pre-selected isolates; (iv) to investigate the ability of these agents to induce biochemical defense responses in maize seedlings; and (v) to evaluate the induction of growth in maize seedlings originating from seeds treated with these agents.

2. Materials and methods

2.1 Obtaining of the isolates

The *M. phaseolina* (231) isolate was obtained from the mycological collection of the Instituto Agris/Brazil. Initially, the pathogen was reactivated through inoculation in corn stalks and, after 30 days of incubation, directly isolated microsclerotia were added to Petri dishes containing PDA (potato - dextrose - agar, 4% w/v). The cultures were incubated in a growth chamber at 25 ± 1°C with a photoperiod of 12h of light at 40 µmol photons m^{-2} s^{-1} for seven days. Subsequently, a monosporic culture was obtained as described by Rajput et al. (2025).

A total of twelve fungal isolates and forty-seven bacterial isolates were obtained from the Laboratório de Fitopatologia do Centro Estadual de Diagnóstico e Pesquisa Agronômica da Secretaria da Agricultura, Pecuária, Produção Sustentável e Irrigação do Rio Grande do Sul (CEAGRO/SEAPI/RS), from the Lavras mycological collection (CML) and from the companies Agrobiológica®, Lallemand®, Simbiose®, Biotrop®, Balagro®, and Koppert® (Online Resource 1). Additionally, an isolate of *Trichoderma virens* (Miller, Giddens & Foster) Arx (1987), obtained from kiwi stem (*Actinidia deliciosa* A. Chev.) infected by *Ceratocystis fimbriata* (Ellis & Halsted, 1890), was included in the bioprospecting. To obtain isolates

from commercial products, an aliquot of each product was spread on Petri dishes containing PDA medium for fungi and TSA medium (tryptic - soy - agar, 2% w/v) for bacterial isolates.

2.2 Molecular identification of *M. phaseolina*

The molecular identification of the *M. phaseolina isolate* was performed by amplifying the Internal Transcribed Spacer (ITS) of the nuclear rDNA. Genomic DNA was extracted from mycelium obtained from colonies grown on PDA medium for seven days, following the Wizard Genomic DNA Purification Kit® protocol (Promega, Madison, WI, USA). PCR reactions were performed in a final volume of 25 µL (3 µL of genomic DNA; 14.5 µL of nuclease-free water; 2.5 µL of PCR buffer (10 ×); 0.75 µL of $MgCl_2$ (50 mM); 0.5 µL of dNTPs (10 mM); 1.25 µL of GoTaq® DNA polymerase (Promega, Madison, WI, USA), and 1.25 µL of each primer (forward and reverse). The amplification and sequencing conditions for the ITS4– ITS5 are shown in Table 1. Amplifications were carried out in a thermocycler (Applied Biosystems, QIAampler 96, Germany). The PCR reaction products were purified using 2 µL of ExoSAP-ITTm (TermoFisher, Santa Clara, USA) following the manufacturer's instructions. Molecular identification was done by comparison with sequences deposited in GenBank (NCBI https://www.ncbi.nlm.nih.gov/genbank/) using the BLASTn (Basic Local Alignment Search Tool nucleotide) algorithm.

Table 1
Conditions for amplification and sequencing of ITS1, ITS4, and ITS5 regions of *Macrophomina phaseolina* 231

Locus	Primers	Sequence (5'–3')	Direction	Initial denaturation	Denaturation (35 cycles)	Annealing	Extension	Final extension	Reference
* ITS									
	ITS5F	GGA AGT AAA AGT CGT AAC AAG G	forward	94°C – 3”	94°C – 45'	55°C – 30”	72°C – 90'	72°C – 10”	White et al. (1990)
	ITS4R	TCC TCC GCT TAT TGA TAT GC	reverse	94°C – 3”	94°C – 45'	55°C – 30”	72°C – 90'	72°C – 10”	White et al. (1990)
*ITS: Internal Transcribed Spacer									

2.3 Antagonism of BCAs

The antagonism of fungal isolates against *M. phaseolina* was evaluated using the double culture technique (Bell et al., 1982). Mycelial discs of 5 mm in diameter, obtained from colonies of *M. phaseolina* and from seven-day-old BCAs, were positioned on opposite sides of Petri dishes containing PDA medium, 2 cm from the inner edge of the plate. The control treatment consisted of plates containing only the mycelial disc of *M. phaseolina*. The plates were incubated in a growth chamber at 25 ± 1°C, under a photoperiod of 12 h of light at 40 µmol s^{-1} m^{-2} for seven days. After incubation, the antagonism was assessed using a rating scale (Bell et al., 1982).

The antagonism of the bacterial isolates was evaluated as previously described (Chandra et al., 2024). The bacterial isolates were initially cultured in TSA medium for 24 h. A 5 mm mycelial disc of *M. phaseolina* was placed per plate (9 cm in diameter) containing PDA medium. The disks were positioned at one end of the plates. At a distance of 4.5 cm, a seeding line of the bacterial isolate was made. The control treatment consisted of plates containing only the mycelial disc of the pathogen. The plates were incubated in a growth chamber at 25 ± 1°C, under a photoperiod of 12 h light at 40 µmol s^{-1} m^{-2} for seven days. The antagonism was assessed using the rating scale of Perneel et al. (2007).

Additionally, the percentage of mycelial growth inhibition (MGI) was determined, according to Rahman et al. (2009), and the mycelial growth rate index (MGRI), according to Maguire (1962). For this, the diameter of *M. phaseolina colonies* was measured daily at two equidistant points using a digital caliper (Electronic digital caliper, Mitutoyo Corporation, Kawasaki, Japan). The fungal and bacterial isolates that exhibited the greatest inhibition of *M. phaseolina* mycelial growth were selected for subsequent assays.

2.4 Antibiosis by BCAs volatile (VOCs) and non-volatile organic compounds (NVOCs)

The selected isolates were evaluated for their ability to inhibit the growth of *M. phaseolina* by producing VOCs and NVOCs. To obtain the non-volatile metabolites, the fungal isolates were cultivated as previously described (Meena et al., 2017). Five mycelial discs of 5 mm in diameter, obtained from seven-day-old cultures of the antagonists, were transferred to sterile Erlenmeyer flasks containing 150 mL of 2% (w/v) PD (potato - dextrose). Flasks were incubated for six days at 25°C, under agitation of 200 rpm. Bacterial isolates were cultured in 4% (w/v) TSB medium (tryptic - soy - broth) for 48 h at 30°C under agitation of 200 rpm (Abdullah et al., 2008). After incubation, the fungal and bacterial cultures were filtered through sterile cheesecloth, centrifuged the 8,000 × *g* for 15 min, and the supernatant was filtered through a 0.22 µm membrane. Aliquots of the filtrate of 250, 350, and 400 mL were incorporated into 1 L of melted PDA poured into Petri dishes. Then, a mycelial disc of 5 mm of *M. phaseolina* was deposited at the center of each plate. The control treatments consisted of plates containing PDA medium supplemented with the same volume of sterile water. The plates were incubated at 25 ± 1°C under a 12 h light photoperiod at 40 µmol m^{-2} s^{-1} for seven days.

The effect of VOCs was evaluated using the Petri dish method. The plates were stacked on top of each other. In the center of the base of the plates containing PDA medium, a 5 mm mycelial disc of *M. phaseolina* was added. On the lid of the plate containing PDA or TSA medium, a disc of the fungal antagonist or a 10 µL aliquot of the bacterial suspension were deposited, respectively. The control treatment consisted of overlapping plates containing the pathogen on the base and lid, with no antagonist. The plates were stacked, sealed with parafilm, and incubated at 25 ± 1°C, under a 12h light photoperiod at 40 µmol m^{-2} s^{-1}.

The mycelial growth of *M. phaseolina* was evaluated daily for seven days by measuring the diameter of the colonies at two equidistant points using a digital caliper (Electronic digital caliper, Mitutoyo Corporation, Kawasaki, Japan). The data obtained were used to calculate the MGRI and MGI.

2.5 Hyperparasitism by fungal BCAs

The pre-selected fungal isolates were evaluated regarding hyperparasitism on *M. phaseolina*. The mycelia of the antagonist and the pathogen were added on opposite sides onto a glass slide containing a thin layer of AA medium (agar - water, 4% w/v). Slides containing only the pathogen mycelium were used as a control. The slides were then placed on Petri dishes containing filter paper previously moistened with distilled sterile water to establish a moist chamber. The plates were closed and incubated in growth cabinet at 25 ± 1°C, under a photoperiod of 12 h light at 40 µmol s^{-1} m^{-2} for 48 h. Hyperparasitism was assessed using a Leica DMR HC microscope (Leica Microsystems, Germany) equipped with a Zeiss Axiocam HRC digital camera (Zeiss Microscopy, Germany).

2.6 Inoculation of corn seeds

Corn seeds of the K9606 VIP3 genotype were previously subjected to emergence and health tests to identify the physiological and sanitary quality of the seeds, according to the Regras para Análise de Sementes (Brazil, 2009). After the tests, the seeds were disinfected in 2% sodium hypochlorite for 1 min, rinsed three times with sterile distilled water, and air-dried for 24 h. Part of the disinfected seeds was inoculated with *M. phaseolina*. For seed inoculation, PDA medium was prepared using a water restriction method by adding mannitol to obtain an osmotic potential of -1.2 MPa (Veiga et al., 2026). Next, 15 mL portions of the PDA medium were poured into Petri dishes and inoculated with 5 mm mycelial discs of *M. phaseolina* at the center of the plates. The plates were incubated in a growth chamber at 25 ± 1°C under a photoperiod of 12 h of light at 40 µmol s^{-1} m^{-2} for seven days. After this incubation period, 30 seeds were distributed in each plate, remaining in contact with the pathogen for 48 h. After incubation, the seeds were removed from the Petri dishes and left to dry in a laminar flow chamber for 24 h.

2.7 Corn seed treatments

Infected and healthy seeds were treated with pre-selected BCAs. The fungal BCAs were subcultured onto PDA medium and incubated in a growth chamber at 25 ± 1°C, under a 12 h of light at 40 µmol s^{-1} m^{-2} for seven days. Sterile distilled water containing 1% Tween 20 was added to the plates, and a superficial scraping of the colonies with a sterile Drigalski loop was performed to obtain a spore suspension. The suspension was filtered through a double layer of sterile gauze, and the concentration adjusted to 1×10^7 spores mL^{-1} in a Neubauer chamber.

The bacterial BCAs were cultured on TSA medium for 24 h at 30°C in the dark. For the preparation of the bacterial suspension, sterile mineral water containing 1% Tween 20 was added to the plates, and the surface of the colonies was scraped with a sterile Drigalski loop. The concentration of the suspension was adjusted to OD_{600nm}= 1, using a spectrophotometer (BEL Engineering, UV-Vis UVM51, Monza, Italy).

Infected and healthy seeds were distributed in Petri dishes and treated with spore or bacterial cell suspensions at a ratio of 10 $mL.kg^{-1}$ of seeds. For the control treatments, infected and healthy seeds received 10 $mL.kg^{-1}$ of sterile distilled water containing 1% Tween 20. After application, the plates were manually agitated for 1 min and kept open until completely dry.

2.8 Resistance Induction by BCAs

Infected seeds treated with pre-selected BCAs, healthy and treated seeds, and healthy and untreated seeds were evaluated. Fifteen seeds from each treatment were sown on germination paper distributed in five repetitions, according to the Regras para Análise de Sementes (Brazil, 2025). The seeds were incubated in a growth chamber at 25 ± 1°C, with a photoperiod of 12 h of light at 40 µmol s^{-1} m^{-2}. Samples were collected at 24, 48, 72 and 96 hours after incubation (hai) and stored at -80°C.

The samples were ground in an electric grinder (Oster, OMDR 110, Ningbo, China) with the addition of liquid nitrogen until a fine powder was obtained. Then, 0.2 g of the ground plant material was added to 1500 µL of extraction buffer (750 µL of 200 mM potassium phosphate buffer, pH 7.8; 15 µL of 10 mM EDTA; 150 µL of 200 mM ascorbic acid; 585 µL of MilliQ water and 10% polyvinylpyrrolidone) and centrifuged at 11,000 × *g* for 20 min at 4°C. The supernatant (enzymatic extract) was stored at -80°C. The quantification of total soluble proteins was done using the Bradford method (1976), with the results expressed in µg of protein mg^{-1} fresh mass. The readings were carried out in a microplate spectrophotometer (Varioskan ™ LUX, Thermo Fisher Scientific, USA) at 595 nm.

Catalase (CAT) activity was determined using a reaction mixture composed of 500 µL of potassium phosphate buffer at 200 mM, pH 7.0; 437.5 µL of Milli-Q water; 12.5 µL of the enzymatic extract; 50 µL of hydrogen peroxide at 250 mM. Aliquots of 190 µL were transferred to 96-well plates, and readings were taken using a microplate spectrophotometer by measuring the decrease in absorbance at 240 nm for 90 s at 25°C. Enzymatic activity was expressed in µmol H_2O_2 min^{-1} mg^{-1} protein.

Superoxide dismutase (SOD) activity was determined based on the ability of the enzyme to inhibit the photoreduction of nitrotetrazolium blue (NBT), according to Giannopolitis & Ries (1977). The reaction mixture consisted of 10 µL of enzyme extract and 190 µL of the reaction mix (100 µL of potassium phosphate buffer at 100 mM, pH 7.8; 40 µL of methionine at 70 mM; 3 µL of EDTA at 10 mM; 15 µL of NBT at 1 mM; 2 µL of riboflavin at 200 µm and 30 µL of Milli-Q water). Aliquots of 190 µL were transferred to 96-well plates and exposed to intense illumination for 3 min and 40 s. After incubation, absorbance was determined at 560 nm. SOD activity was expressed in U SOD min^{-1} mg^{-1} protein, with one unit of SOD considered the amount of enzyme required to promote 50% inhibition of NBT photoreduction.

Phenylalanine ammonia-lyase (PAL) activity was determined according to the protocol described by El-Shora (2002). For each reaction, 9 µL of the crude enzyme extract were added to 161 µL of the reaction mixture (110 µL of 40 mM Tris-HCl buffer, pH 8.8 and 51 µL of 87.5 mM L - phenylalanine). The reactions were incubated at 37°C for 60 min, and trans-cinnamic acid formation was monitored by the increase in absorbance at 290 nm using a microplate spectrophotometer. Enzyme activity was calculated using the molar extinction coefficient of 104 mM^{-1} cm^{-1} (Zucker, 1965) and expressed as U min^{-1} mg^{-1} protein.

2.9 Induction of plant growth by BCAs

The induction of corn seedling growth from seeds infected and treated with pre-selected BCAs and from healthy treated seeds was evaluated. Healthy, untreated seeds served as a control treatment. Two hundred seeds from each treatment, distributed in four replicates of 50 seeds, were sown in trays containing sterile sand, according to the Regras para Análise de Sementes, with minor adaptations (Brazil, 2025). The experiment was conducted in a greenhouse, under an average temperature of 30°C and 55% RH, with daily irrigation to maintain substrate moisture close to saturation. Fifteen days after sowing, the shoot dry biomass (SDB) and root dry biomass (RDB) were determined. For this, the seedlings were sectioned at the insertion point of the first root, separating the shoot and root parts. The samples were placed in kraft paper bags and dried in a forced-air oven at 60 ± 1°C until constant weight.

2.10 Experimental design and statistical analysis

The experiments were conducted in a completely randomized design with four biological replicates, except for the NVOCs assays and enzymatic analyses, which were performed with five biological replicates, with absorbance readings performed in quadruplicate (technical replicates). For the NVOCs assay, the experiment was conducted in a 3 × 6 factorial scheme for fungal isolates and 3 × 13 for bacterial isolates, corresponding to NVOCs concentrations × number of isolates tested. In the enzymatic analyses, the experiment was conducted in a 2 × 5 × 4 factorial scheme, corresponding to seeds infected or not with *M. phaseolina* × number of isolates tested × time after sowing. For the seedling vigor assay, the experiment was conducted in a 2 × 5 factorial scheme, corresponding to seeds infected or not with *M. phaseolina* × number of isolates tested.

The data were evaluated for normality of residuals and homogeneity of variances using the Shapiro–Wilk and Bartlett tests, respectively. Data that met the assumptions of parametric analysis were subjected to analysis of variance (ANOVA), and the means were compared using the Scott-Knott test ($p \leq 0.05$). For the enzymatic analysis data, Welch's t-test ($p \leq 0.05$) was applied to compare seeds infected or not with *M. phaseolina*. Data that did not comply with the assumptions of parametric analysis were analyzed using the Kruskal-Wallis test. For the MGI parameter, multiple paired comparisons were performed for the bacterial isolates, with Holm adjustment ($p \leq 0.05$). For the fungal isolates, the means were transformed according to Box & Cox (1964) using the estimated λ parameter to conform with the assumptions of parametric analysis. The MGI of the NVOCs was analyzed using generalized linear models (GLM). Gaussian, Gamma, and Poisson distributions were evaluated, and the most suitable model was selected based on the Akaike Information Criterion (AIC). When a significant effect was detected, the adjusted means were grouped using the Scott-Knott test ($p \leq 0.05$). All statistical analyses were performed using R software (version 4.3.1), and the graphs were created using GraphPad Prism software (version 9.0).

3. Results

3.1 Molecular identification of *M. phaseolina*

Amplifications of the ITS4–ITS5 regions of *M. phaseolina* resulted in sequences of 565 nucleotides (nt). Comparison of the *amplicons* with sequences available on the GenBank platform, using the BLASTn algorithm, showed high similarity to *M. phaseolina*, with 99.29% identity for MW591609.1. The molecular identification was consistent with the morphological characteristics observed in culture medium. The ITS sequences of *M. phaseolina* were deposited in GenBank under accession numbers PZ439293.1 and PZ439032.1.

3.2 Antagonism of BCAS

All fungal isolates reduced the mycelial growth of *M. phaseolina* in a double culture assay ($p < 0.001$; Fig. 1a–c). However, *T. harzianum* (CCT 7589) and *T. asperellum* (ASN 60) showed the highest MGI, with reductions of approximately 34%, both classified with a score of 2 on the Bell et al. (1982) scale (Fig. 1b). The fungal isolates *T. virens* (FAGRO 1), *T. asperelloides* (MMBF 94/17), and *T. harzianum* (IBLF 006) also showed high antagonistic capacity, with MGI greater than 30%, receiving scores of 1, 1, and 2, respectively. *T. endophyticum* (IBCB 56/12) and *T. harzianum* (Esalq 1306) exhibited intermediate inhibition, both with a score of 2. All fungal isolates also reduced the MGRI of *M. phaseolina*, with *T. harzianum* (CCT 7589) showing the greatest inhibition (Fig. 1c). The MGI and MGRI varied between the *T. harzianum* and *T. asperelloides* isolates, demonstrating that the

antagonistic response was isolate-dependent (Fig. 1b, c). In addition to competition for space and nutrients, antibiosis was observed in most *Trichoderma* isolates, characterized by the formation of inhibition halos, except for *T. endophyticum* (IBCB 56/12) (Fig. 1a).

Nineteen bacterial isolates inhibited the mycelial growth of *M. phaseolina.* ($p < 0.05$; Online Resource 2; Table 2). Among the isolates, *B. subtilis amyloliquefaciens* (ASN 09) and *B. velezensis* (OQ268070.1 and OQ268068.1) presented the highest MGI, exceeding 29%, and were classified with scores of 1, 2, and 2, respectively, according to the scale proposed by Perneel et al. (2007). Akin to what was recorded to fungal BCAs, bacterial isolates of the same species showed variation in mycelial inhibition, demonstrating that the MGI of *M. phaseolina* is dependent on the isolate.

Table 2
Percentage of mycelial growth inhibition (MGI) of *Macrophomina phaseolina* 231 by bacterial biocontrol agents and its classification (score) according to the scale proposed by Perneel et al. (2007)

Isolated	MGI (%)	Notes
Bacillus velezensis (OQ268070.1)	39.5 ± 0.6 ^{a*}	2
B. subtilis amyloliquefaciens (ASN 09)	30.6 ± 0.5 ^{a}	1
B. velezensis (OQ268068.1)	29.0 ± 0.6 ^{ab}	2
B. amyloliquefaciens (ASN 61)	27.5 ± 0.5 ^{bc}	2
B. velezensis (OQ268069.1)	21.8 ± 0.4 ^{bc}	2
B. subtilis (ASN 14)	26.7 ± 0.9 ^{cd}	2
B. siamensis (ASN 47)	26.1 ± 0.3^{de}	2
B. amyloliquefaciens (OQ268078)	25.8 ± 0.6^{de}	2
Priestia megaterium (ASN 22)	25.2 ± 0.3 ^{ef}	2
B. subtilis amyloliquefaciens (ASN 38)	24.4 ± 0.5 ^{fg}	2
B. velezensis (ASN 31)	23.8 ± 0.9 ^{gh}	2
Undefined (ASN 72)	23.1 ± 0.9 ^{hi}	1
Streptomyces violaceus (ASN 39)	22.8 ± 0.4 ^{hi}	2
B. methylotrophicus (UFPEDA 20)	22.5 ± 0.5 ^{ij}	2
B. subtilis (ASN 37)	22.2 ± 1.5 ^{jk}	1
B. subtilis amyloliquefaciens (ASN 06)	21.7 ± 0.6 ^{jk}	2
B. amyloliquefaciens (ASN 50)	21.3 ± 0.7 ^{kl}	1
B. amyloliquefaciens SIMBI BS 10 (CCT 7600)	21.6 ± 0.4 ^{kl}	1
Undefined (ASN 73)	18.4 ± 0.4 ^{lm}	1
B. subtilis (ASN 44)	6.4 ± 0.3 ^{m}	0
B. cereus (ASN 01)	0.0 ± 0.0 ^{n}	0
B. cereus (ASN 07)	0.0 ± 0.0 ^{n}	0
B. cereus (ASN 18)	0.0 ± 0.0 ^{n}	0
B. cereus (ASN 20)	0.0 ± 0.0 ^{n}	0
B. pumilus (ASN 49)	0.0 ± 0.0 ^{n}	0
B. pumilus (ASN 13)	0.0 ± 0.0 ^{n}	0
B. safensis (OQ303893)	0.0 ± 0.0 ^{n}	0
B. subtilis amyloliquefaciens (ASN 36)	0.0 ± 0.0 ^{n}	0
B. licheniformis (ASN 12)	0.0 ± 0.0 ^{n}	0
Bacillus sp. (ERC 3.3)	0.0 ± 0.0 ^{n}	0
Bacillus sp. (ES7)	0.0 ± 0.0 ^{n}	0
B. tequilensis (ASN 48)	0.0 ± 0.0 ^{n}	0

*Values are presented as mean ± standard deviation (n = 4). Identical letters indicate the absence of a significant difference between treatments, according to the Kruskal-Wallis test, followed by multiple comparisons with Holm adjustment ($p < 0.05$)

Isolated	MGI (%)	Notes
B. thuringiensis (ASN 17)	0.0 ± 0.0 [n]	0
B. thuringiensis (ASN 45)	0.0 ± 0.0 [n]	0
B. thuringiensis aizawai (ASN 71)	0.0 ± 0.0 [n]	0
B. thuringiensis var. *kurstaki* (ASN 52)	0.0 ± 0.0 [n]	0
B. thuringiensis var. *kurstaki* (ASN 08)	0.0 ± 0.0 [n]	0
B. wiedmanni (OQ304003)	0.0 ± 0.0 [n]	0
Serratia marcescens (ASN 03)	0.0 ± 0.0 [n]	0
Streptomyces griseoviridis (K61)	0.0 ± 0.0 [n]	0
Pseudomonas putida reidholzensis (ASN 27)	0.0 ± 0.0 [n]	0
Pseudomonas fluorescens (ASN 15)	0.0 ± 0.0 [n]	0
Priestia aryabhattai (ASN 10)	0.0 ± 0.0 [n]	0
Priestia aryabhattai (ASN 40)	0.0 ± 0.0 [n]	0
Priestia megaterium (ASN 46)	0.0 ± 0.0 [n]	0
Undefined (ASN 74)	0.0 ± 0.0 [n]	0
Undefined (ASN 75)	0.0 ± 0.0 [n]	0

*Values are presented as mean ± standard deviation (n = 4). Identical letters indicate the absence of a significant difference between treatments, according to the Kruskal-Wallis test, followed by multiple comparisons with Holm adjustment ($p < 0.05$)

3.3 Antibiosis by BCAs volatile (VOCs) and non-volatile organic compounds (NVOCs)

T. virens (FAGRO 1), *T. asperelloides* (MMBF 94/17), *T. endophyticum* (IBCB 56/12), *T. asperellum* (ASN 60), *T. harzianum* (CCT 7589), *B. subtilis amyloliquefaciens* (ASN 09), *B. velezensis* (ASN 31; OQ268068.1 and OQ268070.1), *B. amyloliquefaciens* (OQ268078 and ASN 61), *B. methylotrophicus* (UFPEDA 20), *B. siamensis* (ASN 14 and ASN 47), *B. subtilis* (ASN 37), *Streptomyces violaceus* (ASN 39) *Priestia megaterium* (ASN 22), and *Priestia megaterium* (ASN 22) were selected for these assays because they exhibited higher antagonistic capacity in double culture against *M. phaseolina.* There was a significant interaction between the isolates and the concentrations of NVOCs of fungal BCAs on the MGI and MGRI of *M. phaseolina* ($p < 0.001$; Fig. 2a–c). *T. asperellum* (ASN 60) showed the highest antifungal activity, especially at doses of 350 and 400 $mL.L^{-1}$, with inhibitions of 29 and 37.8%, respectively (Fig. 2a, b). *T. virens* (FAGRO 1), at a dose of 400 $mL.L^{-1}$, also showed high inhibition of *M. phaseolina* mycelial growth (32.3%). *T. asperellum* (ASN 60) at the lowest dose evaluated, *T. asperelloides* (MMBF 94/17) and *T. endophyticum* (IBCM 56/12) at a dose of 400 $mL.L^{-1}$, showed intermediate inhibitions (20–24%). *T. asperelloides* (MMBF 94/17), at a dose of 350 $mL.L^{-1}$, and *T. harzianum* (CCT 7589) at the lowest doses had low inhibitory effect, with values below 15%. The MGRI corroborated the MGI results (Fig. 2c). The lowest MGRI values were observed for *T. asperellum* (ASN 60) at all doses evaluated, as well as for *T. virens* (FAGRO 1) at a dose of 400 $mL.L^{-1}$. *T. harzianum* (CCT 7589) showed MGRI values comparable to the controls, indicating low NVOC activity on *M. phaseolina*.

VOCs from *Trichoderma species* reduced the MGI and MGRI of *M. phaseolina* ($p < 0.001$; Fig. 3a–c). *T. asperellum* (ASN 60) and *T. endophyticum* (IBCM 56/12) promoted the greatest inhibition of mycelial growth, greater than 31% (Fig. 3b). Intermediate inhibition was observed for *T. asperelloides.* (MMBF 94/17), with a reduction of 22.2%, followed by *T. virens* (FAGRO 1) with 12.9%. *T. harzianum* (CCT 7589) showed the lowest inhibitory effect (8.8%). The MGRI corroborated the MGI results (Fig. 3c).

There was a significant interaction between the isolates and the concentrations of crude extracts of bacterial BCAs on the MGI and MGRI of *M. phaseolina* ($p < 0.001$; Fig. 4a–c). *B. amyloliquefaciens* (ASN 61) showed the greatest antifungal effect, promoting inhibition of *M. phaseolina* growth greater than 95% and MGRI values close to zero, even at the lowest dose (Fig. 4b, c). *B. velezensis* (OQ268068.1) also demonstrated high antifungal activity at all concentrations, with inhibition greater than 80% and a marked reduction in MGRI. *B. methylotrophicus* (UFPEDA 20) had equivalent performance to *B. velezensis* (OQ268068.1) only at the highest concentration. *B. amyloliquefaciens* (OQ268078) and *B. subtilis* (ASN 14) showed intermediate growth reducing effects, especially at the higher doses, with inhibition greater than 60% and a significant reduction in MGRI. Moderate reductions in mycelial growth (6.3–36.1%) were also observed for *B. siamensis* (ASN 47), *B. subtilis amyloliquefaciens* (ASN 09), and *B. velezensis* (OQ268070.1), with intermediate MGRI values. The other treatments did not differ statistically from the controls.

The VOCs of the bacterial isolates reduced the MGI and MGRI of *M. phaseolina* (Fig. 5a–c; $p < 0.001$). The greatest reduction in MGI was observed for *B. subtilis* (ASN 37), with 37.8% inhibition (Fig. 5a, b; $p < 0.001$). *P. megaterium* (ASN 22) and *S. violascens* (ASN 39) also showed high percentages of inhibition (circa 35%). *B. siamensis* (ASN 47) showed intermediate inhibition (30.7%), as did *B. methylotrophicus* (UFPEDA 20), *B. subtilis amyloliquefaciens* (ASN 09), *B. velezensis* (ASN 31), *B. velezensis* (OQ268068.1), and *B. velezensis* (OQ268070.1) (25–27%). *B. amyloliquefaciens* (OQ268078), *B. amyloliquefaciens* (ASN 61) and *B. subtilis* (ASN 14) showed the lowest MGI, although still higher than the control. The MGRI data corroborated the MGI results (Fig. 5c; $p < 0.001$).

3.4 Hyperparasitism by fungal BCAs

Antagonistic interactions typical of hyperparasitism were observed between the five pre-selected *Trichoderma* isolates and *M. phaseolina* (Fig. 6a–e). Directional growth of *Trichoderma*, accompanied by coiling around the hyphae of *M. phaseolina* and the formation of hook-like structures, were observed mainly in *T. virens* (FAGRO 1), *T. asperellum* (ASN 60), and *T. harzianum* (CCT 7589). *T. asperelloides* (MMBF 94/17) and *T. endophyticum* (IBCB 56/12) predominantly showed hyphal contact and hyphal aggregation.

3.5 Resistance Induction by BCAs

There was a significant interaction between uninfected and *M. phaseolina* infected seeds, BCAs, and time after treatment for the activity of CAT, SOD, and PAL ($p < 0.001$; Fig. 7a–f). Overall, CAT activity was relatively stable over time but increased at 96h in all treatments (Fig. 7a, b). In infected seeds, higher CAT activity was observed at 96 h when treated with *B. subtilis amyloliquefaciens* (ASN 09) and *T. harzianum* (CCT 7589) (Fig. 7a). In uninfected seeds, differences were observed only at 72 and 96 ha, with an increase in CAT in seeds treated with *T. asperellum.* (ASN 60) and *T. harzianum* (CCT 7589) at 72h and reduction at 96h with *T. harzianum* (CCT 7589) treatment (Fig. 7b). Comparing uninfected seeds to those infected with *M. phaseolina*, both having been treated with the BCAs, higher CAT activity was observed at 24h in uninfected seeds treated with *T. asperellum* (ASN 60), and in infected seeds treated with *T. harzianum* (CCT 7589) (Fig. 7a, b). At 48 h, infected seeds treated with *B. velezensis* (OQ268070.1) showed higher CAT activity compared to uninfected seeds treated with the same BCA. At 72 h, uninfected seeds treated with *T. asperellum* (ASN 60) and *T. harzianum* (CCT 7589) showed higher CAT activity compared to those infected and treated with the same BCAs. At 96 h, infected seeds treated with *T. harzianum* (CCT 7589) and *B. velezensis* (OQ268070.1) showed higher CAT activity, while uninfected seeds treated with *T. asperellum* showed higher CAT activity. Seeds untreated with BCAs, had higher CAT activity when uninfected. Not infected seeds treated with *T. asperellum* (ASN 60) and *B. subtilis amyloliquefaciens* (ASN 09) showed increased CAT activity compared to their infected counterparts. Overall, infected seeds treated *B. velezensis* (OQ268070.1) and *B. subtilis amyloliquefaciens* (ASN 09) showed the largest increases.

SOD activity tended to increase over time, regardless of infection with *M. phaseolina* or the application of BCAs; however, infected seeds treated with *T. asperellum* (ASN 60), *T. harzianum* (CCT 7589), and *B. velezensis* (OQ268070.1) showed higher increases (Fig. 7c, d). In infected seeds, differences were observed at 24 and 96 h, with increased SOD in untreated seeds and seeds treated with *T. asperellum* (ASN 60), *T. harzianum* (CCT 7589), and *B. velezensis* (OQ268070.1), respectively (Fig. 7c). In uninfected seeds, differences between treated and untreated seeds were observed only at 96 h, with reduced SOD in treated seeds. Comparing infected and uninfected seeds at 24 h, higher SOD was observed in infected seeds treated with *T. harzianum* (CCT 7589), and higher SOD in uninfected seeds treated with *B. velezensis* (OQ268070.1) (Fig. 7c, d). At 48 h, higher SOD was observed in uninfected seeds treated with *T. asperellum* (ASN 60), *B. subtilis amyloliquefaciens* (ASN 09) and *B. velezensis* (OQ268070.1), compared to infected seeds treated with the same BCAs. At 72 h, no differences were observed between infected and uninfected seeds for all treatments. However, at 96h, higher SOD was observed in infected seeds treated with *T. harzianum* (CCT 7589), and in uninfected and untreated seeds.

PAL activity increased over time, regardless of *M. phaseolina* infection or BCAA application. (Fig. 7e, f). The largest overall increase of PAL activity in infected seeds was observed with *B. subtilis amyloliquefaciens* (ASN 09), whereas in uninfected seeds, *B. velezensis* (OQ268070.1) and *B. subtilis amyloliquefaciens* (ASN 09) promoted enzymatic activity the most. In infected seeds, differences between treated and untreated seeds were observed only at all sampling times (Fig. 7e). At 48 h, a reduction in PAL was observed in seeds treated with BCAs compared to untreated seeds. However, at 72 h, PAL increased in seeds treated with *T. harzianum* (CCT 7589) and *B. velezensis* (OQ268070.1). At 96 h the enzyme activity augmented in seeds treated with *B. subtilis amyloliquefaciens* (ASN 09). In uninfected seeds, differences between treatments were observed at 24, 48, and 96 h. At 24 h, an increase in PAL was observed with *T. asperellum* (ASN 60) and *T. harzianum* (CCT 7589) (Fig. 7f). At 48 h, a reduction in PAL was observed in seeds treated with BCAs. At 96 h, an increase in PAL was observed in seeds treated with *B. velezensis* (OQ268070.1) and *B. subtilis amyloliquefaciens* (ASN 09). Comparing infected and uninfected seeds at 24 h, higher PAL activity was observed in uninfected seeds treated with *T. asperellum* (ASN 60) and *T. harzianum* (CCT 7589), and in infected seeds that were untreated and treated with *B. velezensis* (OQ268070.1). At 48 h, higher PAL activity was observed in infected seeds, whether treated or not, compared to uninfected seeds in all treatments. At 72 h, higher PAL activity was observed in infected seeds treated with *T. harzianum* (CCT 7589) and *B. velezensis* (OQ268070.1), compared to their uninfected seeds counterparts. At 96 h, higher PAL activity was observed in uninfected seeds treated with *B. velezensis* (OQ268070.1), compared to infected seeds treated with the same BCA.

3.7 Induction of plant growth by BCAs

There was a significant interaction between infected and uninfected seeds and the BCAs on the SDB and RDB of maize seedlings ($p < 0.001$; Fig. 8a–c). Infection with *M. phaseolina* reduced SDB and RDB in seedlings originating from untreated seeds (Fig. 8b, c). However, all BCAs increased SDB and RDB in seedlings originating from infected seeds. For SDB, the highest values were observed with *T. harzianum* (CCT 7589) (Fig. 8b). For RDB, the highest values were observed with *T. asperellum* (ASN 60) and *T. harzianum* (CCT 7589) (Fig. 8c). In seedlings originating from healthy seeds and

treated with BCAs, *T. harzianum* (CCT 7589) and *B. velezensis* (OQ268070.1) promoted the increases of SDB the most (Fig. 8b). The other treatments did not promote an increase in SDB. For RDB, all BCAs promoted biomass accumulation, with the highest values observed in seeds treated with *T. harzianum* (CCT 7589), *B. subtilis amyloliquefaciens* (ASN 09), and *B. velezensis* (OQ268070.1) (Fig. 8c).

3.8 Mechanisms of action of BCAs on *M. phaseolina*

BCA isolates showed diverse mechanisms of action in suppressing *M. phaseolina* (Table 3). Among the fungal isolates, *T. asperellum* (ASN 60) presented the broadest profile, combining high antagonism in dual culture, strong inhibition by NVOC and VOC-mediated antibiosis, hyperparasitism, and redox modulation. *T. harzianum* (CCT 7589) showed high antagonism in dual culture and hyperparasitism, associated with redox modulation and promotion of SDB and RDB. Among the bacterial isolates, *B. velezensis* (OQ268070.1) presented the broadest and most multifaceted profile of mechanisms of action, combining high antagonism in dual culture, intermediate antibiosis by VOCs and NVOCs, redox modulation, high PAL activity, and stimulation of SDB and RDB increases. *B. subtilis amyloliquefaciens* (ASN 09) showed high antagonism in double culture, intermediate antibiosis by VOCs and NVOCs, high PAL activity and increased RDB in uninfected seedlings.

Table 3 Characterization of the direct and indirect mechanisms of action of biocontrol agents in the suppression of *Macrophomina phaseolina in vitro* and in corn seedlings

Isolated	CD	NVOCs	VOCs	H	CAT (I)	CAT (NI)	SOD (I)	SOD (NI)	PAL (I)	PAL (NI)	SDB (I)	SDB (NI)	RDB (I)	RDB (NI)	Predominant mechanisms of action
Bacillus amyloliquefaciens (ASN 61)	++	+++	+	–	nd	nd	nd	nd	nd	nd	nd	nd	nd	nd	Antibiosis by NVOCs
B. amyloliquefaciens (OQ268078)	++	+++	+	–	nd	nd	nd	nd	nd	nd	nd	nd	nd	nd	Antibiosis by NVOCs
B. methylotrophicus (UFPEDA 20)	++	+++	+	–	nd	nd	nd	nd	nd	nd	nd	nd	nd	nd	Antibiosis by NVOCs
B. siamensis (ASN 14)	++	+++	+	–	nd	nd	nd	nd	nd	nd	nd	nd	nd	nd	Antibiosis by NVOCs
B. siamensis (ASN 47)	++	++	++	–	nd	nd	nd	nd	nd	nd	nd	nd	nd	nd	Antibiosis caused by VOCs + NVOCs
B. subtilis (ASN 37)	++	+	+++	–	nd	nd	nd	nd	nd	nd	nd	nd	nd	nd	Antibiosis due to VOCs
B. subtilis amyloliquefaciens (ASN 09)	+++	++	++	–	+	++	+	++	+++	++	++	++	++	+++	Antibiosis by VOCs + NVOCs + PAL + RDB
B. velezensis (OQ268068.1)	+++	+++	+	–	nd	nd	nd	nd	nd	nd	nd	nd	nd	nd	Antibiosis by NVOCs
B. velezensis (OQ268070.1)	+++	++	+	–	+++	++	+++	++	++	+++	+++	+++	+	+++	Antibiosis by NVOCs + redox + PAL + SDB
B. velezensis (ASN 31)	++	+	+	–	nd	nd	nd	nd	nd	nd	nd	nd	nd	nd	Competition
Streptomyces violaceus (ASN 39)	++	+	++	–	nd	nd	nd	nd	nd	nd	nd	nd	nd	nd	Antibiosis due to VOCs
Priestia megaterium (ASN 22)	++	+	++	–	nd	nd	nd	nd	nd	nd	nd	nd	nd	nd	Antibiosis due to VOCs
Trichoderma asperellum (ASN 60)	+++	+++	+++	+++	++	++	+++	++	++	+	++	+	+++	++	Antibiosis by VOCs + EB + M + *redox* + RDB
T. harzianum (CCT 7589)	+++	+	+	+++	+++	++	+++	+	+	++	+++	+++	+++	+++	Competition + M + *redox* + SDB + RDB
T. endophyticum (IBCB 56/12)	++	+	+++	+++	nd	nd	nd	nd	nd	nd	nd	nd	nd	nd	Antibiosis by VOCs + M
T. asperelloides (MMBF 94/17)	++	+	++	+++	nd	nd	nd	nd	nd	nd	nd	nd	nd	nd	Antibiosis by VOCs + M
T. virens (FAGRO 1)	++	++	+	+++	nd	nd	nd	nd	nd	nd	nd	nd	nd	nd	Antibiosis by NVOCs + M

The symbols indicate the relative intensity of each mechanism: +++ = high activity; ++ = intermediate activity; + = low activity; – = mechanism not observed or not applicable; nd = not determined. CD = double culture method; NVOCs = non-volatile organic compounds; VOCs = volatile organic compounds; H = hyperparasitism; CAT = catalase; SOD = superoxide dismutase; PAL = phenylalanine ammonia-lyase; I = seedlings originating from seeds infected with *M. phaseolina*; NI = seedlings originating from uninfected seeds. The agents that showed the highest inhibition capacity in double culture were highlighted and subsequently evaluated for growth promotion and resistance induction

4. Discussion

Trichoderma asperellum (ASN 60), *T. harzianum* (CCT 7589), *B. subtilis amyloliquefaciens* (ASN 09) and *B. velezensis* (OQ268070.1) stood out among the 59 BCAs evaluated, showing high potential for the control of *M. phaseolina*. The results indicate that the antagonistic activity of these isolates results from the integrated action of different direct mechanisms of action, such as the production of antimicrobial compounds and/or hyperparasitism, and indirect mechanisms, related to the modulation of biochemical defense responses and the promotion of maize seedling growth.

The high inhibition of *M. phaseolina* mycelial growth promoted by *T. harzianum* (CCT 7589) and *T. asperellum* (ASN 60) in the double culture assay suggests that direct antagonism mechanisms play a central role in the interaction between these BCAs and the phytopathogen. Among these mechanisms, competition for space and nutrients, hyperparasitism, and the secretion of lytic enzymes capable of degrading structural components of the fungal cell wall, such as chitinases, β-1,3- glucanases, and proteases have been observed (Manzar et al., 2021). These characteristics are well known for *Trichoderma* species and may have contributed to the significant inhibition of mycelial growth of *M. phaseolina* observed in the present study. Among the bacterial isolates, *B. subtilis*, *B. amyloliquefaciens* (ASN 09) and *B. velezensis* (OQ268070.1 and OQ268068.1) promoted the highest levels of pathogen inhibition in double culture. This performance is associated with a combination of competition for resources and the production of antimicrobial metabolites. Species belonging to the *B. subtilis complex* are recognized for their ability to synthesize lipopeptides, such as surfactins, iturins, and fengycins, as well as VOCs, capable of disturbing growth and cellular integrity of phytopathogenic fungi (Luo et al., 2022; Dutilloy et al., 2026).

The variation in *M. phaseolina* inhibition observed among isolates of the same species supports the fact that biocontrol effectiveness depends mainly on the functional characteristics of the specific isolate rather than its taxonomic identity. Indeed, genetically close isolates may present contrasting responses against the same pathogen. Intraspecific differences in metabolite production, antagonistic activity, and environmental adaptation have been reported for *Trichoderma* and *Bacillus* (Ghanbarzadeh et al., 2014; Jayanti et al., 2025). These differences likely reflect the genetic, metabolic, and physiological variation that influences the deployment of mechanisms of action and the adaptation of isolates to different environments and pathosystems (Geng et al., 2025). Thus, the results reinforce that the selection of BCAs should be based on the functional characterization of each isolate, and not exclusively on taxonomic identification.

Assays with VOCs and NVOCs showed that the select isolates exhibit distinct metabolic antagonism strategies. *Trypanosoma asperellum* (ASN 60) was able to inhibit pathogen growth through both VOCs and NVOCs, suggesting the capacity to produce a broad repertoire of antifungal metabolites. The antifungal activity of this species has been associated with the production of compounds such as hydroxytoluene, butylated propylene glycol, hexadecanoic acid, 9- octadecenoic acid, and ergosterol (Elshahawy & Marrez, 2023). Although the antagonistic activity of *T. endophyticum* against *M. phaseolina* has already been reported in double culture assays (Veiga et al., 2026), studies evaluating the effect of VOCs against the pathogen were missing. *T. endophyticum* showed increased activity mediated by VOCs than by NVOCs, indicating that volatile compounds may represent an important component of its mechanism of action. This species is known for its biosynthetic potential, having multiple gene clusters related to the production of secondary metabolites (Castro et al., 2023).

Trichoderma harzianum (CCT 7589) presented a distinct functional profile compared to the other isolates evaluated. Despite its low antifungal activity mediated by VOCs and NVOCs, it strongly inhibited mycelial growth of *M. phaseolina* in a double culture assay and displayed significant hyperparasitic activity like other *Trichoderma* species. These results suggest that its antagonistic efficiency relies primarily on mechanisms that require direct interaction with the pathogen, such as competition for space and nutrients and hyperparasitism. Similar results were reported by Ghanbarzadeh. et al. (2014) who observed high suppression capacity of *T. harzianum* on *Fusarium* sp., even in the absence of strong activity mediated by diffusible metabolites. The authors attributed the supressive activity to the establishment of physical contact between antagonist and pathogen and the subsequent induction of hydrolytic enzymes. This behavior can be particularly relevant in environments where physical contact between antagonist and pathogen is favored, such as in the rhizosphere and on seed surfaces.

Whereas the antagonism of the fungi appeared to depend mostly on the direct interaction with the pathogen, the results suggest that suppression promoted by *B. velezensis* e *B. subtilis amyloliquefaciens* was more related to the production of antimicrobial metabolites. *B. velezensis* (OQ268070.1 and OQ268068.1) showed significant suppressive activity associated with NVOCs and moderately with VOCs. In contrast, *B. subtilis amyloliquefaciens* (ASN 09) had higher VOC- mediated activity, indicating distinct metabolic strategies among isolates belonging to the same taxonomic group. These isolates belong to the *B. subtilis* complex, currently included in the operational group *B. amyloliquefaciens*, recognized for its high capacity for rhizosphere colonization and the production of a wide repertoire of secondary metabolites (Fan et al., 2017). Previous studies demonstrate that species of this group can synthesize lipopeptides, polyketides, and different VOCs with antifungal and biostimulant activity (Luo et al., 2022). However, the composition and concentration of these metabolites vary significantly between isolates and are strongly influenced by culture conditions (Raza et al., 2016).

In addition to antagonistic activity against *M. phaseolina*, the pre-selected bacterial and fungal isolates promoted the growth of maize seedlings, highlighting their multifunctional potential. However, the observed effects differed among the isolates, suggesting that distinct physiological mechanisms may be involved in promoting plant growth. *T. asperellum* promoted shoot growth, without a significant effect on the root system. On the other hand, *T. harzianum* (CCT 7589) promoted an increase in both SDB and RDB of corn seedlings. This effect may be related to the production of *Trichoderma* secondary metabolites capable of modulating hormonal and physiological processes in the plant. Examples of such metabolites include sesquiterpenes, alcohols, molecules involved in development signaling processes, and phytohormones, which may result in increased growth (Matar et al., 2022). *B. velezensis* (OQ268070.1) increased SDB, whereas *B. subtilis amyloliquefaciens* (ASN 09) promoted RDB. These results suggest functional specializations among the isolates evaluated and agree with studies that demonstrate the ability of species of the *B. amyloliquefaciens* group to promote plant growth through different mechanisms, including siderophore production, auxin synthesis, nutrient solubilization, and emission of bioactive VOCs (Luo et al., 2022; Ilyas et al., 2024).

In addition to directly suppressing *M. phaseolina* and promoting growth in maize, the selected BCAs induced changes in the biochemical responses of maize seedlings derived from both healthy and infected seeds. This observation suggests that the BCAs action also involves the modulation of defense responses. The changes observed in the activity of antioxidant enzymes and PAL showed strong temporal dependence, indicating that the plant-pathogen-BCA interaction constitutes a dynamic process, in which different defense pathways are activated along the infection progress. More pronounced increases in CAT at 96 h were observed, while SOD and PAL exhibited specific patterns between treatments throughout the evaluated period. Temporal changes in defense responses are well known. In interactions involving susceptible genotypes, the activation of antioxidant systems and structural defenses tends to occur later when compared to resistant genotypes (Chowdhury et al., 2017). This aspect is relevant considering the absence of known corn genotypes resistant to charcoal rot (Harlapur et al., 2024). The observed temporal dynamics may also be related to the infection strategies of *M. phaseolina*. Recent studies demonstrate that this pathogen produces enzymes with functional similarity to plant enzymes, potentially capable of delaying or modulating initial recognition by the host (Shirai & Eulgem, 2023). On the other hand, the reduction in enzymatic activity in subsequent periods does not necessarily represent a weakening of the defensive response, but rather a process of physiological adjustment after the initial establishment of defense barriers. In fact, this is a frequently described profile in induced resistance processes (Walters et al., 2013). Thus, the modulation of these responses by BCAs may represent a complementary protective mechanism, contributing to reducing the effects of stress caused by pathogen colonization.

Among the treatments of infected seeds, *T. harzianum, T. asperellum*, and *B. velezensis* promoted an increase in SOD and CAT activities at 96 h. This pattern suggests a coordinated modulation of the antioxidant system, favoring the balance between ROS production and detoxification during the plant-pathogen interaction (Mittler, 2016; Wang et al., 2018). The combined action of these enzymes may contribute to maintaining signaling concentrations of hydrogen peroxide, important for activating defense responses, while simultaneously preventing its excessive accumulation and the resulting oxidative damage (Mittler, 2016). This physiological adjustment may be particularly relevant in interactions involving necrotrophic

pathogens, since the uncontrolled accumulation of ROS favors cell death processes frequently exploited by these organisms during tissue colonization (Govrin & Levine, 2000). Coordinated increases in antioxidant enzymes induced by *Bacillus* species have been described in mung beans (*Vigna radiata* L.) (Hashem et al., 2017) and soybean (Yasmin et al., 2020), while *T. harzianum* has been linked to the activation of the antioxidant system, mainly under abiotic stress conditions (Eftekhari et al., 2025). Pretreatment of tomato seedlings with *T. harzianum* enhanced antioxidant enzyme activities and protected against challenge by the hemibiotrophic pathogen *Fusarium oxysporum* f. sp. *lycopersici* (Zehra et al., 2017).

Increased PAL activity in infected seedlings treated with *B. subtilis amyloliquefaciens* is indicative of the phenylpropanoid pathway activation, responsible for the biosynthesis of a myriad of important defense-related products, including salicylic acid, flavonoids, stilbenes, coumarins, lignin, and several phytoalexins (Kaur et al., 2022; Ramaroson et al., 2022). The accumulation of phenylpropanoid pathway derivatives may lead to concerted structural strengthening of the cell wall and production of antimicrobial compounds, thereby restricting the progression of colonization by *M. phaseolina*. The predominance of this response in treatments with *B. subtilis amyloliquefaciens* suggests a stronger association of this isolate with the activation of structural and metabolic defense mechanisms in the host, reinforcing its role as an inducer of systemic resistance in maize.

In seedlings originating from uninfected seeds, enzymatic patterns suggest that BCAs promoted physiological adjustments consistent with the establishment of a metabolic priming state. The transient increase in CAT activity in seedlings treated with *T. asperellum* and *T. harzianum* indicates modulation of oxidative metabolism, affording a balance between H_2O_2 signaling and oxidative damage impact (Geng et al., 2025). In contrast, the higher SOD activity in control seedlings may reflect a basal condition of redox homeostasis, without the physiological reprogramming normally induced by the plant-beneficial microorganism interaction (Mittler, 2016). Metabolic priming consists of the host physiological reprogramming, conferring higher speed and efficiency to subsequent stress responses (Francioli et al., 2025). Similar results have been described in healthy plants in different pathosystems involving *Bacillus* spp. (Yasmin et al., 2020; Chauhan et al., 2022). PAL activity increase in seedlings derived from seeds treated with *B. velezensis and B. subtilis amyloliquefaciens* suggests early activation of the phenylpropanoid pathway, consistent with a metabolic priming state. This pattern is also in line with studies that associate *Bacillus* spp. with the induction of PAL, polyphenol oxidase (PPO), and peroxidase (POD) activities (Luo et al., 2022). Similar results were reported by Zhang et al. (2020) with healthy soybean plants treated with *T. harzianum.* Thus, whereas in the absence of the pathogen BCAs may promote preventive metabolic reprogramming, under infection conditions these microorganisms could lead to rapid activation of the same pathways to modulate defense.

Taken together, data suggest that the evaluated BCAs act through complementary mechanisms. While the production of antifungal metabolites and direct antagonism could reduce the initial establishment of *M. phaseolina*, the modulation of antioxidant responses and the phenylpropanoid pathway would increase the plant's ability to respond to the infectious process. This functional complementarity likely represents one of the main factors responsible for the high efficiency observed for the select isolates, reinforcing that biological control results from the concerted interactions among physiological processes of all the players involved.

Whereas *B. subtilis amyloliquefaciens* (ASN 09) showed stronger association with the activation of the phenylpropanoid pathway, *T. harzianum* (CCT 7589), *T. asperellum* (ASN 60), and *B. velezensis* (OQ268070.1) predominantly modulated the antioxidant system. Biocontrol agents capable of combining direct antagonism, production of bioactive metabolites, promotion of plant growth, and modulation of plant defense responses tend to exhibit high functional robustness, reduced dependence on a single suppression mechanism, and low probability of resistance development, potentially increasing the stability of control under different environmental conditions. (Zehra et al., 2017; Luo et al., 2022). Future investigations should focus on characterizing the bioactive metabolites associated with biocontrol and growth promotion, as well as validating these agents under field conditions and in integrated disease management programs.

This study expands the knowledge about the multifunctional mechanisms involved in the interaction between isolates of *Trichoderma*, *Bacillus*, maize, and *M. phaseolina*, demonstrating that the efficiency of BCAs results from the integration between microbial antagonism, biochemical modulation of the plant, and promotion of plant growth. In addition to identifying promising isolates for the management of maize smut rot, the results contribute to advancing knowledge on the complex interaction of the triad plant-pathogen-beneficial microorganism.

5. Conclusions

Trichoderma harzianum (CCT 7589), *T. asperellum* (ASN 60), *Bacillus velezensis* (OQ268070.1) and *B. subtilis amyloliquefaciens* (ASN 09) constitute promising isolates for the control of *M. phaseolina* in corn. The antagonistic activity of *Trichoderma* species was mainly associated with a combination of competition, hyperparasitism, and antibiosis mediated by volatile and non-volatile bioactive metabolites, whereas the bacterial isolates acted predominantly via antibiosis. In addition to direct antagonism, all biocontrol agents promoted modulation of biochemical responses and stimulation of initial maize growth. *T. harzianum* (CCT 7589), *T. asperellum* (ASN 60) and *B. velezensis* (OQ268070.1) were associated with modulation of the antioxidant system, while *B. velezensis* (OQ268070.1) and *B. subtilis amyloliquefaciens* (ASN 09) were related to activation of the phenylpropanoid pathway. These effects were accompanied by increased shoot growth induced by *T. harzianum.* (CCT 7589) and *B. velezensis* (OQ268070.1), and promotion of root development by *T. asperellum* (ASN 60), *T. harzianum* (CCT 7589), *B. subtilis amyloliquefaciens* (ASN 09), and *B. velezensis* (OQ268070.1) in healthy seedlings.

Declarations

Author contributions Jayne D. da Veiga: conceived and designed the study, performed the sampling, processed and analyzed the data, and wrote the paper. Fábio A. Antonelo: performed the sampling and processed and analyzed the data. Arthur G. Fett-Neto: contributed to study design, reviewed drafts, wrote the paper and contributed with reagents/materials/analysis tools. Andréia Mara R. de Oliveira wrote the paper. André C. da Silva: conceived and designed the study, reviewed drafts, wrote the paper and contributed with reagents/materials/analysis tools. All authors read and approved the final manuscript.

Funding This study was supported by the Coordenação de Aperfeiçoamento de Pessoal de Nível Superior (CAPES – finance code 001), the Fundação de Amparo à Pesquisa do Estado do Rio Grande do Sul (FAPERGS – 25/2551-0000954-5), and Conselho Nacional de Pesquisa e Desenvolvimento Tecnológico (CNPq – grant number 310775/2021-3).

Acknowledgments The authors also thank Prof. Dr. Roberto Lanna Filho, Prof. Lauri Lourenço Radunz, and Deila Magna dos Santos for their assistance and contributions during the development of this study. The authors are grateful to Agrobiológica Soluções Biológicas, Lallemand Plant Care, Instituto Agris, and Supra Sementes for providing biological products and seed materials that supported the development of this research.

Data availability The datasets generated and/or analyzed during the current study are available in the Zenodo repository at 10.5281/zenodo.21086855 .

Conflict of interest The authors declare that they have no known competing financial interests or personal relationships that could have appeared to influence the work reported in this paper.

References

1. Abdullah TM, Ali NY, Suleman P (2008)Biological control of *Sclerotinia sclerotiorum* (Lib.) de Bary with *Trichoderma harzianum* and *Bacillus amyloliquefaciens.* Crop Prot 27(10):1354–1359. 10.1016/j.cropro.2008.05.007
2. AGROFIT. Ministério da Agricultura e Pecuária (2026) Available at: https://www.gov.br/agricultura/pt–br/assuntos/insumos-agropecuarios/insumos- agricultural / pesticides / agrofit. Accessed on 04/01/2026
3. Ahmed MJ, Shoaib A (2024) Unveiling the biocontrol potential of *Pseudomonas syringae* through seed biopriming against charcoal rot disease in maize. Physiol Mol Plant Pathol 133:102370. 10.1016/j.pmpp.2024.102370
4. Arx, JA von. (1987) Plant pathogenic fungi. Beihefte zur Nova Hedwigia 87(1):288. 10.5555/19871326377
5. Bell DK, Wells HD, Markham CR (1982) *In vitro* antagonism of *Trichoderma* species against six fungal plant pathogens.Phytopathology 72(4):379–382. Available from: https://www.apsnet.org/publications/phytopathology/backissues/Documents/1982Articles/Phy to72n04_379.PDF. Access on 10/05/2024
6. Bradford MM (1976) A rapid and sensitive method for the quantification of microgram quantities of protein utilizing the principle of protein-dye binding.Anal Biochem 72 (1/2):248–254. 10.1016/0003-2697(76)90527-3
7. BRAZIL (2025) Ministério da Agricultura, do Abastecimento e da Reforma Agrária. Secretaria Nacional de Defesa Agropecuária. Regras para Análise de Sementes.2nd ed. Brasília – DF. MAPA. Available at: https://wikisda.agricultura.gov.br/pt-br/Laborat%C3%B3rios/Metodologia/Sementes/RAS_2025/Amostragem .
8. Box GEP, Cox DR (1964) An analysis of transformations. JR Stat Soc Ser A Stat Soc: Series B (Methodological) 26(2):211–243. 10.1111/j.2517-6161.1964.tb 00553.x
9. Castro GS et al (2023) Characterization of peptaibols produced by a marine strain of the fungus *Trichoderma endophyticum* via mass spectrometry, genome mining and phylogeny-based prediction. Metabolites 13:221. 10.3390/metabo13020221
10. Chandra P et al (2024) *Bacillus subtilis* strain BS87as a biocontrol agent against spot blotch disease: effect on growth, nutrient status, and antioxidant enzymes in wheat.Acta Physiol Plant 46:35. 10.1007/s11738–024–03657–5
11. Chauhan P et al (2022) *Bacillus subtilis* suppresses the charcoal rot disease by inducing defense responses and physiological attributes in soybean. Arch Microbiol 204:266. 10.1007/s00203–022–02876–z
12. Chowdhury S, Basu A, Kundu S (2017) Biotrophy-necrotrophy switch in pathogen evoke differential response in resistant and susceptible sesame involving multiple signaling pathways at different phases. Sci Rep 7(1):17251. 10.1038/s41598–017–17248–7
13. Deboni da Veiga J et al (2026) Bioprospecting and characterization of the mechanisms of action of *Trichoderma* and *Bacillus* species against *Macrophomina phaseolina* in maize [Data set]. Zenodo. 10.5281/zenodo.21086855 .
14. Dutilloy E et al (2026) Lipopeptide-mediated antagonism: Modulation of *Bacillus velezensis* strain BE2 lipopeptides in response to *Zymoseptoria tritici* and *Pyrenophora teres*. Microbiological Research 309:128514. 10.1016/j.micres.2026.128514 .
15. Halsted BD (1890) Some fungal diseases of the sweet potato. Bulletin New Jersey Agricultural Experiment Station 76:7–14. 10.1079/cabicompendium.12143
16. El–shora *HM (2002) Properties of phenylalanine ammonia-lyase from marrow cotyledons.Plant Sci 162(1):1–7. 10.1016/S0168-9452(01)00471-X*
17. Elshahawy IE, Marrez DA (2024) Antagonistic activity of *Trichoderma asperellum* against *Fusarium* species, chemical profile and its efficacy for management of *Fusarium* -root rot disease in dry bean. Pest Manag Sci 80:1153–1167. 10.1002/ps.7846

18. Eftekhari F et al(2025) Effects of mycorrhizal and *Trichoderma* treatment on enhancing maize tolerance to salinity and drought stress, through metabolic and enzymatic evaluation. BMC Plant Biol 25:687. 10.1186/s12870-025-06729-x
19. Fan B et al. (2017) *Bacillus amyloliquefaciens*, *Bacillus velezensis*, and *Bacillus siamensis* form an "Operational Group *B. amyloliquefaciens*" within the *B. subtilis* species complex. Frontiers in Microbiology 8:22. 10.3389/fmicb.2017.00022
20. Francioli D et al (2025) Microbial inoculants modulate the rhizosphere microbiome, alleviate plant stress responses, and enhance maize growth at field scale. Genome Biol 26:148. 10.1186/s13059-025-03621-7
21. Geng Y et al (2025) Positive role of *Trichoderma harzianum* in increasing plant tolerance to abiotic stresses: a review. Antioxidants 14:807. 10.3390/antiox14070807
22. Giannopolitis CN, Ries SK (1977) Superoxide dismutases: I. Occurrence in higher plants. Plant Physiol 59(2):309–314. 10.1104/pp.59.2.309
23. Goidanich G (1947) Revision the genre *Macrophomina* Petrak. Typical species: *Macrophomina phaseolina* (Tass.) Goid. nov. comb. nec. *M. phaseoli*. Ann Speriment Agrar 1:449–461. Available at: https://eurekamag.com/research/013/623/013623418.php#:~:text=Now%20for%20$29.90-,Summary,genus%20and%20species%20are%20given . Accessed on 02/05/2024
24. Ghanbarzadeh B, Safaie N, Goltapeh EM (2014) Antagonistic activity and hyphal interactions of *Trichoderma* spp. against *Fusarium proliferatum* and *F. oxysporum in vitro*.Arch Phytopathol Plant Prot 47(16):1979–1987. 10.1080/03235408.2013.864506
25. Govrin EM, Levine A (2000) The hypersensitive response facilitates plant infection by the necrotrophic pathogen *Botrytis cinerea*. Curr Biol 29;10(13):751–7. 10.1016/s0960-9822(00)00560-1
26. Graphpad software: GraphPad Prism (2021) version 9.0 for [Mac]. GraphPad Software, San Diego, California, USA. Available at: www.graphpad.com . Accessed on 01/11/2025.
27. Harlapur SI, Khokhar MK, Hooda KS (2024) Epidemiology and management of corn smut caused by *Macrophomina phaseolina* (Tassi.) Goid. In: Kumar P, Dubey RC *Macrophomina phaseolina*: Ecobiology, Pathology and Management. Academic Press, 135–145.
28. Hashem A et al (2017) Plant defense approach *Bacillus subtilis* (BERA 71) against *Macrophomina phaseolina* (Tassi) Goid in mung bean. J Plant Interact 12:390–401. 10.1080/17429145.2017.1373871 .
29. Ilyas T et al (2024) Exploring the potentiality of *Bacillus amyloliquefaciens* as a prominent biocontrol agent: a comprehensive overview.In Microorganisms for Sustainability 1:133–150. 10.1007/978-981-99-8195-3_7 .
30. Jayanti RM et al (2025) Bioprospecting of Plant -Beneficial *Bacillus* species for growth promotion and disease suppression. Trop Life Sci Res 36(2):1–21. 10.21315/tlsr2025.36.2.1.
31. Kaur S et al (2022) How do plants defend themselves against pathogens-biochemical mechanisms and genetic interventions.Physiol Mol Biol Plants 28:485–504. 10.1007/s12298-022-01146-y
32. Khalili E et al (2026) Integrated management of charcoal rot (*Macrophomina phaseolina*) in soybean: current strategies and the emerging role of β- glucosidase.Appl Soil Ecol 217:106549. 10.1016/j.apsoil.2025.106549 .
33. Luo L et al (2022) *Bacillus amyloliquefaciens* as an excellent agent for biofertilizer and biocontrol in agriculture: An overview for its mechanisms. Microbiological Research 259:127016. 10.1016/j.micres.2022.127016 .
34. Maguire JD (1962) Speed of germination aid in selection and evaluation for seedling emergence and vigor.Crop Sci 2(2):176–77. 10.2135/cropsci1962.0011183X000200020033x
35. Manzar N et al (2021) Biocontrol potential of native *Trichoderma* spp. against anthracnose of great millet (*Sorghum bicolour* L.) from Tarai and hill regions of India. Biological Control 152:104474. 10.1016/j.biocontrol.2020.104474
36. Marquez N et al (2021) *Macrophomina phaseolina*: general characteristics of pathogenicity and methods of control.Front Plant Sci 12:634397. 10.3389/fpls.2021.634397
37. Matar N et al (2022) Identification of beneficial Lebanese *Trichoderma* spp. wheat endophytes. Front Plant Sci 13:1017890. 10.3389/fpls.2022.1017890
38. Meena M et al (2017) Antagonistic assessment of *Trichoderma spp.* by producing volatile and non-volatile compounds against different fungal pathogens.Arch Phytopathol Plant Prot 50:629–648. 10.1080/03235408.2017.1357360
39. Mittler R (2016) ROS are good. Trends Plant Sci 22(1):11– 9. 10.1016/j.tplants.2016.08.002
40. Perneel M et al (2007) Characterization of CMR5c and CMR12a, novel fluorescent *Pseudomonas* strains from the cocoyam rhizosphere with biocontrol activity.J Appl Microbiol 103(4):1007–1020. 10.1111/j.1365- 2672.2007. 03345.x.
41. Poria V et al (2025) Activation of induced systemic resistance in cotton plants against *Fusarium* and *Macrophomina* by microbial antagonists. J Plant Growth Regul 44:7055–7075. 10.1007/s00344-024-11495-5
42. Rahman MA, Begum MF, Alam MF (2009) Screening of *Trichoderma* isolates as a biological control agent against *Ceratocystis paradoxa* causing pineapple disease of sugarcane. Mycobiology 37:277–285. 10.4489/MYCO.2009.37.4.277
43. Ramaroson ML et al (2022) Role of phenylpropanoids and flavonoids in plant resistance to pests and diseases. Molecules 27:8371. 10.3390/molecules27238371

44. Rajput LS et al (2025) Morpho -cultural, pathogenic, and genetic characterization of Indian isolates of *Macrophomina phaseolina* causing charcoal rot in soybean. Heliyon 17;11(2):42035. 10.1016/j.heliyon.2025.e 42035
45. Raza W et al (2016) Effect of organic fertilizers prepared from organic waste materials on the production of antibacterial volatile organic compounds by two biocontrol *Bacillus amyloliquefaciens* strains.J Biotechnol 227:43–53. 10.1016/j.jbiotec.2016.04.014
46. R Core Team (2021) R:a language and environment for statistical computing. R Foundation for Statistical Computing, Vienna, Austria
47. Shirai M, Eulgem T (2023) Molecular interactions between the soilborne pathogenic fungus *Macrophomina phaseolina* and its host plants.Front Plant Sci 13. 10.3389/fpls.2023.1264569
48. Veiga JD (2026) Biofungicides in the control of charcoal rot and the biochemical and physiological alterations caused in maize genotypes. Dissertation (Master's) – Universidade Federal do Rio Grande do Sul, Faculdade de Agronomia, Graduate Program in Crop Science, Porto Alegre, RS, BR
49. Veiga JD et al (2026) *Trichoderma endophyticum, T. asperellum*, and *T. harzianum* suppress charcoal rot in soybean seeds infected by *Macrophomina phaseolina*. Eur J Plant Pathol. 10.1007/s10658-026-03192-8
50. Walters DR, Ratsep J, Havis ND (2013) Controlling crop diseases using induced resistance: challenges for the future. J Exp Bot 64(5):1263–1280. 10.1093/ jxb /ert026
51. Wang Y et al(2018)Superoxide dismutases: dual roles in controlling ROS damage and regulating ROS signaling.J Cell Biol 217(6):1915–1928. 10.1083/jcb.201708007
52. White TJ, Bruns T, Taylor SL (1990) Amplification and direct sequencing of fungal ribosomal RNA genes for phylogenetics.In: Innis MA et al. (Eds). PCR Protocols: a guide to methods and applications 315–322. 10.1016/B978-0-12-372180-8.50042-1
53. Yasmin H et al(2020)Identification of new biocontrol agent against charcoal rot sisease caused by *Macrophomina phaseolina* in soybean (*Glycine max* L.).Sustainability Sci Practice Policy 12(17):6856. 10.3390/su12176856
54. Zehra A et al (2017) Synergistic effects of plant defense elicitors and *Trichoderma harzianum* on enhanced induction of antioxidant defense system in tomato against Fusarium wilt disease. Bot Stud 58:44. 10.1186/s40529-017-0198-2
55. Zhang F et al (2020) The application potential of *Trichoderma* T- soybean containing 1-aminocyclopropane-1-carboxylate for maize production. Physiol Mol Plant Pathol 110: 101475. 10.1016/j.pmpp.2020.101475
56. Zucker M (1965) Induction of phenylalanine deaminase by light and its relation to chlorogenic acid synthesis in potato tuber tissue. Plant Physiol 40:779–784. 10.1104/pp.40.5.779

Figures

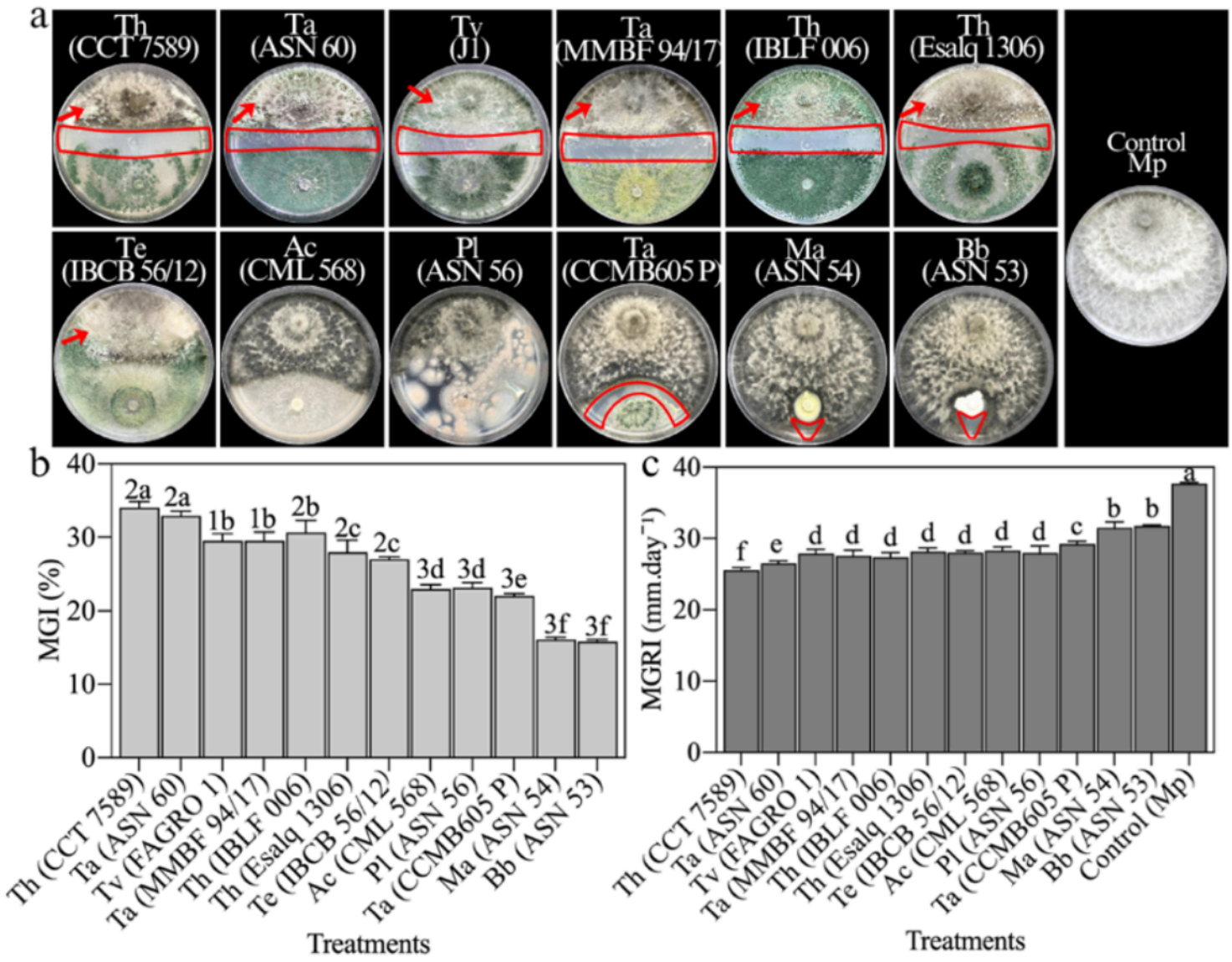


Figure 1

In vitro antagonism of fungal biocontrol agents (BCAs) against *Macrophomina phaseolina* 231 (Mp) after seven days of incubation in culture medium. The BCAs evaluated were *Trichoderma harzianum* (Th; CCT 7589, IBLF 006 and Esalq 1306), *T. asperellum* (Ta ASN60), *T. virens* (Tv FAGRO 1), *T. asperelloides* (Ta MMBF 94/17), *T. endophyticum* (Te IBCB 56/12), *Arthrobotrys cadodores* (Ac CML 568), *Purpureocillium lilacinus* (Pl ASN 56), *Metarhizium anisopliae* (Ma ASN 54) and *Beauveria bassiana* (Bb ASN 53). **(a)** Double culture technique demonstrating the antagonism of BCAs on Mp. Red lines indicate the inhibition halo and arrows highlight the growth of BCAs on the Mp colony. **(b)** Percentage of mycelial growth inhibition (MGI) and **(c)** Mycelial growth rate index (MGRI) of Mp. Values are presented as mean ± standard deviation (n= 4). Numbers above each bar represent scores according to the Bell et al. (1982) scale. Bars with the same letter do not differ according to the Scott-Knott test ($p< 0.001$). For the MGI, the data were transformed according to Box & Cox (1964), using the parameter λ estimated from the data themselves. The averages are presented with the untransformed values

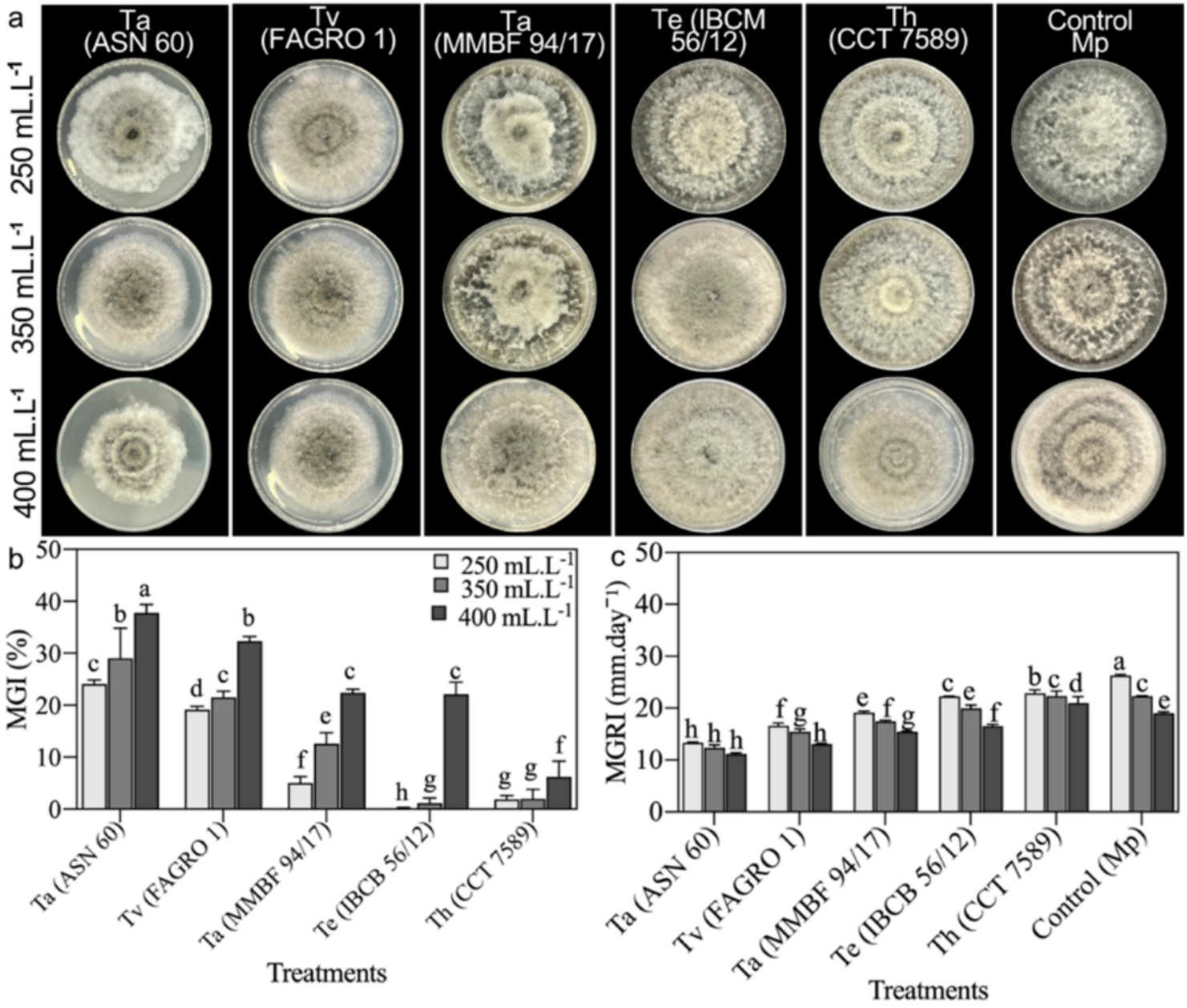


Figure 2

Effect of non-volatile organic compounds (NVOCs) from *Trichoderma asperellum* (Ta ASN 60), *T. virens* (Tv FAGRO 1), *T. asperelloides* (Ta MMBF 94/17), *T. endophyticum* (Te IBCM 56/12), and *T. harzianum* (Th CCT 7589) on the mycelial growth of *Macrophomina phaseolina* 231 (Mp) after seven days of incubation. **(a)** Mycelial growth of Mp in the presence of different concentrations (250, 350, and 400 mL. L^{-1}) of NVOCs. **(b)** Percentage of mycelial growth inhibition (MGI) and **(c)** Mycelial growth velocity index (MGRI) of Mp. Data are presented as mean ± standard deviation (n = 5). Different letters indicate significant differences between treatments, according to the Scott– Knott test ($p< 0.001$). Variables were analyzed using generalized linear models (GLM), followed by the Scott–Knott test

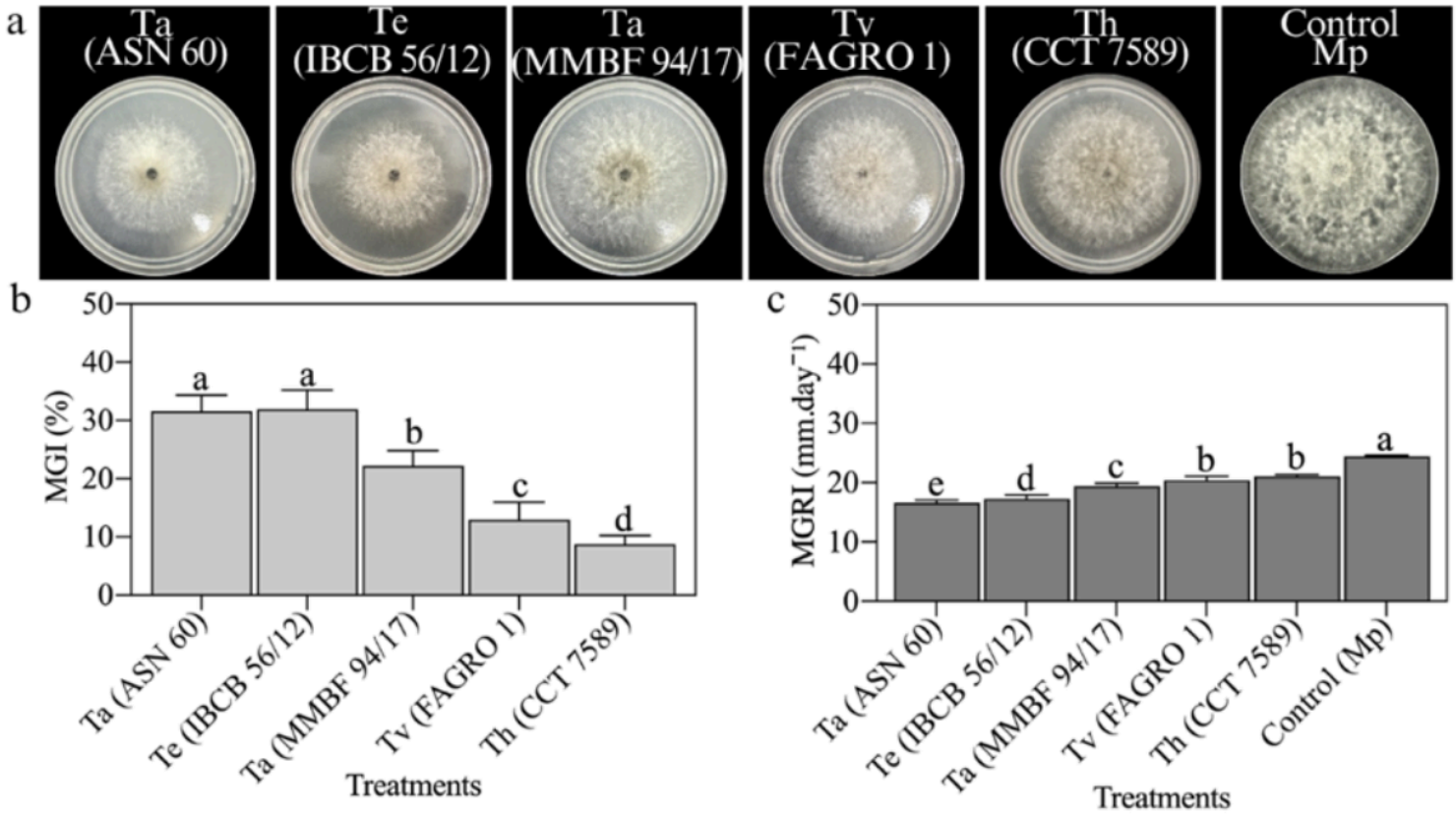


Figure 3

Effect of volatile organic compounds (VOCs) from *T. asperellum* (Ta ASN 60), *T. virens* (Tv FAGRO 1), *T. asperelloides* (Ta MMBF 94/17), *T. endophyticum* (Te IBCM 56/12) and *T. harzianum* (Th CCT 7589) on the mycelial growth of *Macrophomina phaseolina* 231 (Mp) after seven days of incubation. **(a)** Mycelial growth of Mp exposed to volatile metabolites produced by *Trichoderma* isolates. **(b)** Percentage of mycelial growth inhibition (MGI) and **(c)** Mycelial growth rate index (MGRI) of Mp. Values are presented as mean ± standard deviation (n= 4). Different letters indicate significant differences between treatments, according to the Scott-Knott test ($p< 0.001$)

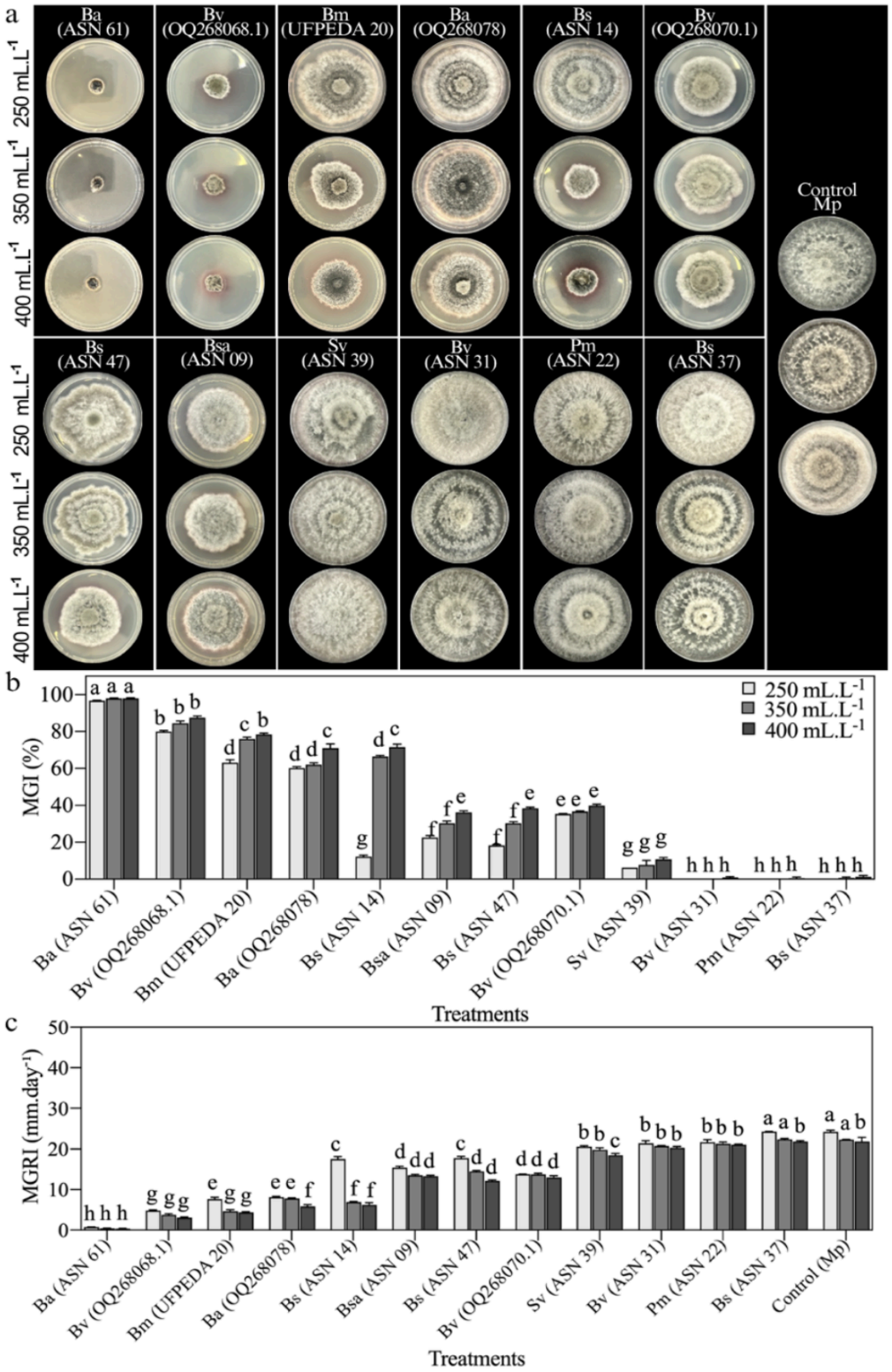


Figure 4

Effect of non-volatile organic compounds (NVOCs) from bacterial biocontrol agents on the mycelial growth of *Macrophomina phaseolina* 231 (Mp) after 7 days of incubation. **(a)** Mycelial growth of Mp in the presence of NVOCs from isolates of *Bacillus amyloliquefaciens* (Ba; ASN 61 and OQ268078), *B. methylotrophicus* (Bm; UFPEDA 20), *B. siamensis* (Bs; ASN 14 and ASN 47), *B. subtilis* (Bs ASN 37), *B. subtilis amyloliquefaciens* (Bsa ASN 09), *B. velezensis* (Bv; OQ268068.1, OQ268070.1, and ASN 31), *Streptomyces violaceus* (Sv ASN 39) and *Priestia megaterium* (Pm ASN 22) at concentrations of 250, 350, and 400 mL.L^{-1}, and control (Mp, no exposure). **(b)** Percentage of mycelial growth inhibition (MGI) and **(c)** Mycelial growth velocity index (MGRI) of Mp. Values are presented as mean ± standard deviation (n= 5). Different letters indicate significant differences between treatments, according to the Scott-Knott test ($p< 0.001$). Variables were analyzed using generalized linear models (GLM), followed by the Scott-Knott test

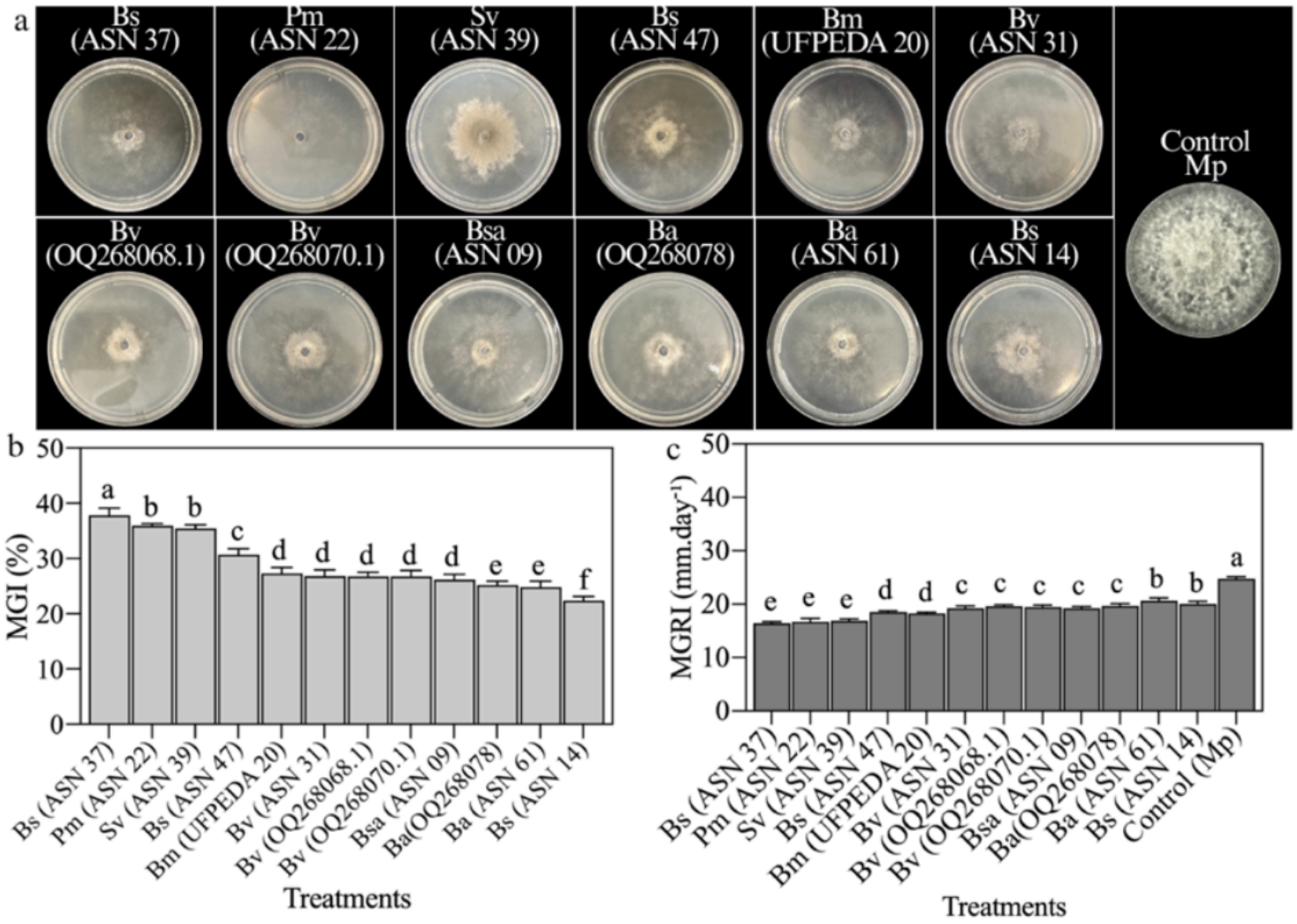


Figure 5

Volatile organic compounds (VOCs) from bacterial isolates on the mycelial growth of *Macrophomina phaseolina* 231 (Mp) after 7 days of incubation. **(a)** Mycelial growth of Mp in the presence of VOCs from *Bacillus amyloliquefaciens* (Ba; ASN 61 and OQ268078), *B. methylotrophicus* (Bm; UFPEDA 20), *B. siamensis* (Bs; ASN 14 and ASN 47), *B. subtilis* (Bs; ASN 37), *B. subtilis amyloliquefaciens* (Bsa; ASN 09), *B. velezensis* (Bv; OQ268068.1, OQ268070.1 and ASN 31), *Streptomyces violaceus* (Sv; ASN 39) and *Priestia megaterium* (Pm; ASN 22), and control (Mp, no exposure). **(b)** Percentage of mycelial growth inhibition (MGI) and **(c)** Mycelial growth velocity index (MGRI) of Mp. Values represent the mean ± standard deviation (n= 4). Different letters indicate significant differences between treatments, according to the Scott-Knott test (p< 0.001)

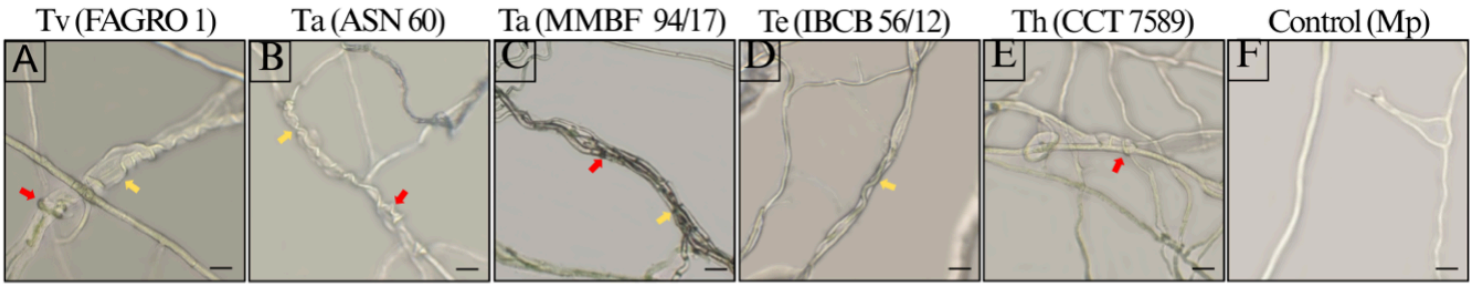


Figure 6

Mycelial interactions between *Trichoderma virens* (Tv FAGRO 1) **(a)**, *T. asperellum* (Ta ASN 60) **(b)**, *T. asperelloides* (Ta MMBF 94/17) **(c)**, *T. endophyticum* (Te; IBCB 56/12) **(d)** and *T. harzianum* (Th CCT 7589) **(e)** with *Macrophomina phaseolina* 231 in microculture after 48h of incubation. **(f)** Hyphae of *M. phaseolina* without interaction with antagonists (Control Mp). The interaction regions show structures associated with hyperparasitism, including hook-like structure formation (red arrows), hyphal coiling of *Trichoderma* around the pathogen hyphae, and hyphal aggregation (yellow arrows). Scale bar= 10 µm

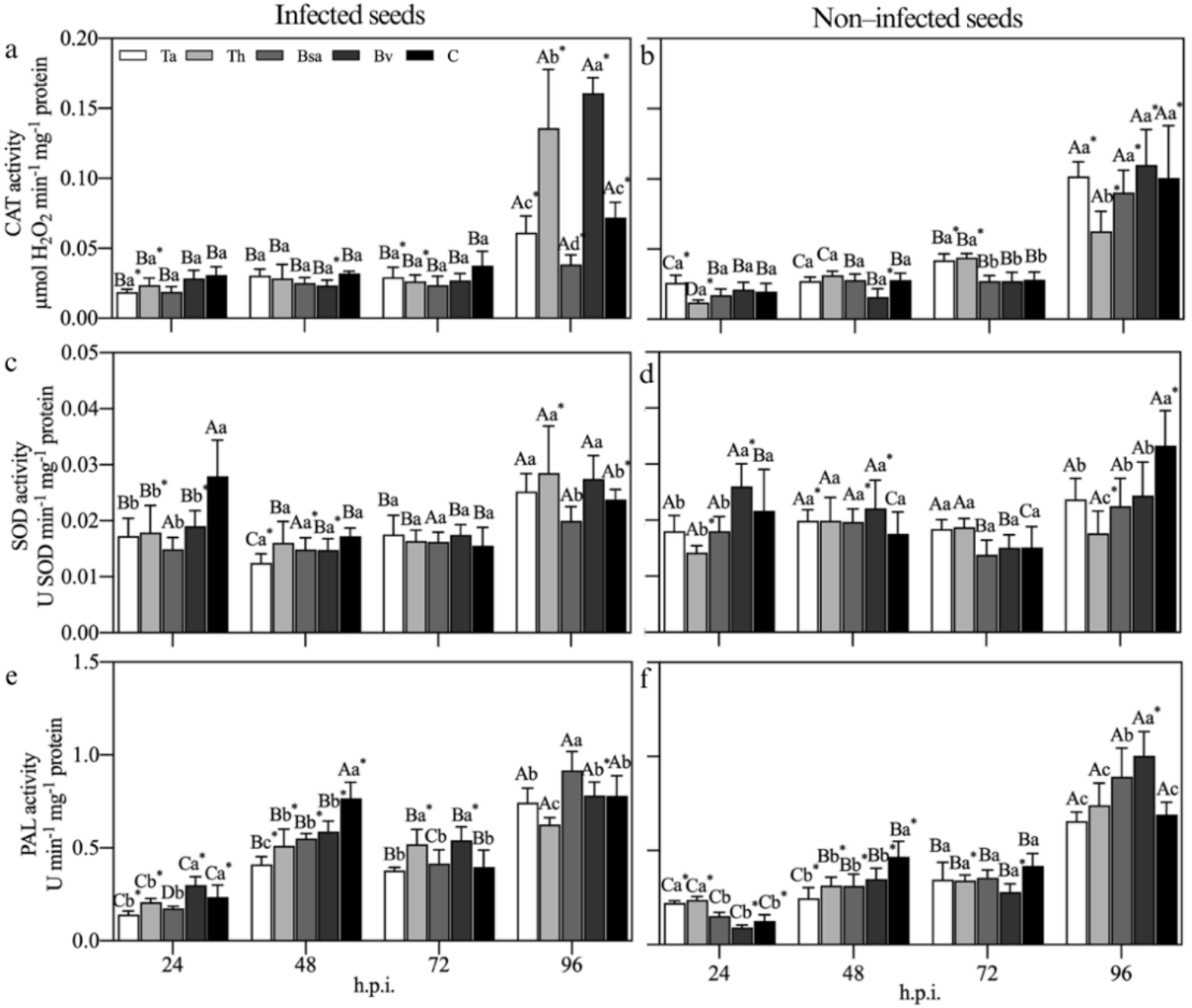


Figure 7

Activity of antioxidant and defense-related enzymes in maize seeds infected or not with *Macrophomina phaseolina* 231 (C) and subjected to treatments with *Trichoderma asperellum* (Ta ASN 60), *T. harzianum* (Th CCT 7589), *Bacillus subtilis amyloliquefaciens* (Bsa ASN 09) and *B. velezensis* (Bv OQ268070.1) at 24, 48, 72 and 96 hours after incubation (hai). (**a, b**) Catalase (CAT) activity; (**c, d**) Superoxide dismutase (SOD) activity; (**e, f**) Activity of Phenylalanine ammonia-lyase (PAL). Values represent the mean ± standard deviation (n= 5). Different lowercase letters indicate significant differences between treatments within each time point, while different uppercase letters indicate differences between evaluation periods for the same treatment, according to the Scott-Knott test ($p < 0.001$). *Indicates a significant difference between infected and uninfected seeds within each treatment, according to Welch's t-test ($p \leq 0.05$)

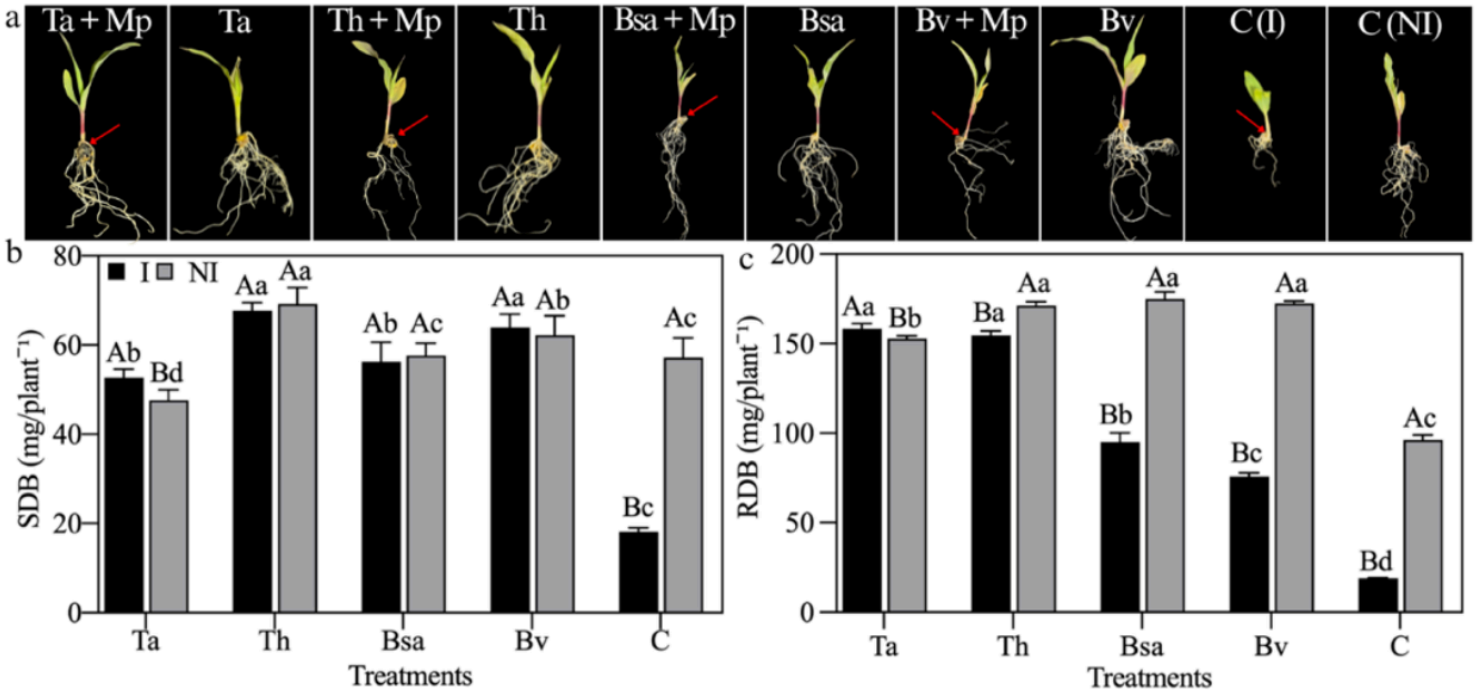


Figure 8

Shoot dry biomass (SDB) and root dry biomass (RDB) of maize seedlings originating from seeds treated with *Trichoderma asperellum* (Ta; ASN 60), *T. harzianum* (Th; CCT 7589), *Bacillus subtilis amyloliquefaciens* (Bsa; ASN 09) and *B. velezensis* (Bv; OQ268070.1), when infected (I) or not (NI) by *Macrophomina phaseolina* 231 (Mp), 15 days after sowing. **(a)** Images of maize seedlings subjected to the treatments. **(b)** SDB values and **(c)** RDB values. Data are presented as mean ± standard deviation (n= 4). Uppercase letters indicate differences between infection conditions within each treatment, and lowercase letters indicate differences between treatments within each infection condition, by the Scott-Knotttest ($p < 0.001$)

Supplementary Files

This is a list of supplementary files associated with this preprint. Click to download.

- SupplementaryInformation2.docx
- Supplementaryinformation1.docx